TABLE 2. Association study using frequent SNPs in *HIF1A* in patients with T2DM and controls

SNP name	Frequencies of minor allele			Frequencies of genotype		T2DM *vs.* control	
	T2DM (n = 440)	Control (n = 572)		T2DM (n = 440)	Control (n = 572)	χ^2	*P*
SNP30	0.144	0.141	W/W	0.736	0.754	0.042	0.837
			W/M	0.240	0.211		
			M/M	0.024	0.035		
SNP31	0.06	0.065	W/W	0.892	0.890	0.195	0.658
			W/M	0.096	0.090		
			M/M	0.012	0.020		
SNP1	0.073	0.072	W/W	0.857	0.859	0.007	0.934
			W/M	0.138	0.138		
			M/M	0.004	0.004		
SNP2	0.127	0.133	W/W	0.759	0.746	0.134	0.714
			W/M	0.228	0.243		
			M/M	0.013	0.011		
SNP3	0.186	0.2	W/W	0.670	0.648	0.553	0.457
			W/M	0.286	0.304		
			M/M	0.043	0.048		
SNP4	0.145	0.147	W/W	0.729	0.733	0.007	0.932
			W/M	0.251	0.241		
			M/M	0.020	0.027		
SNP5	0.146	0.136	W/W	0.725	0.748	0.392	0.532
			W/M	0.257	0.231		
			M/M	0.018	0.021		
SNP6(S28Y)	0.009	0.014	W/W	0.983	0.972	1.141	0.285
			W/M	0.017	0.028		
			M/M	0	0		
SNP25	0.188	0.222	W/W	0.664	0.613	3.465	0.063
			W/M	0.296	0.331		
			M/M	0.040	0.056		
SNP7	0.196	0.225	W/W	0.650	0.606	2.481	0.115
			W/M	0.307	0.338		
			M/M	0.042	0.056		
SNP8	0.148	0.148	W/W	0.721	0.722	0	0.996
			W/M	0.261	0.259		
			M/M	0.018	0.019		
SNP9	0.416	0.429	W/W	0.345	0.312	0.32	0.572
			W/M	0.477	0.518		
			M/M	0.178	0.170		
SNP10(P582S)	0.041	0.073	W/W	0.918	0.863	8.925	**0.003**
			W/M	0.082	0.127		
			M/M	0	0.010		
SNP11(A588T)	0.047	0.044	W/W	0.908	0.917	0.141	0.708
			W/M	0.090	0.080		
			M/M	0.002	0.004		
SNP14	0.126	0.129	W/W	0.760	0.752	0.038	0.846
			W/M	0.228	0.238		
			M/M	0.011	0.009		
SNP15	0.424	0.431	W/W	0.326	0.306	0.12	0.729
			W/M	0.501	0.525		
			M/M	0.173	0.169		
SNP16	0.126	0.129	W/W	0.760	0.752	0.038	0.846
			W/M	0.228	0.238		
			M/M	0.011	0.009		
SNP17	0.126	0.129	W/W	0.760	0.752	0.038	0.846
			W/M	0.228	0.238		
			M/M	0.011	0.009		
SNP18	0.122	0.128	W/W	0.770	0.758	0.194	0.66
			W/M	0.217	0.227		
			M/M	0.013	0.015		
SNP20	0.173	0.199	W/W	0.690	0.643	2.14	0.143
			W/M	0.273	0.316		
			M/M	0.037	0.041		
SNP12	0.135	0.132	W/W	0.742	0.746	0.061	0.804
			W/M	0.245	0.245		
			M/M	0.013	0.009		
SNP13	0.211	0.222	W/W	0.615	0.605	0.314	0.575
			W/M	0.347	0.345		
			M/M	0.038	0.049		
SNP28	0.327	0.335	W/W	0.470	0.465	0.16	0.69
			W/M	0.407	0.400		
			M/M	0.123	0.135		
SNP29	0.109	0.097	W/W	0.799	0.822	0.768	0.381
			W/M	0.183	0.161		
			M/M	0.017	0.017		

P value < 0.05 is shown in *bold*. M, Mutant; W, wild type.

SNP-25	SNP-7	SNP-8	SNP-9	SNP-10 (P582S)	SNP-14	SNP-15	SNP-18	SNP-20	SNP-12	SNP-13	Frequency CONT	Frequency T2DM
1	1	1	1	1	1	1	1	1	1	1	0.537	0.543
1	1	1	2	1	1	2	1	1	1	1	0.213	0.215
2	2	2	2	1	2	2	2	2	2	2	0.108	0.085
2	2	1	2	2	1	2	1	2	1	2	0.070	0.035
2	2	2	2	1	2	2	1	2	2	2	0.017	0.022
2	2	2	1	1	1	1	2	1	1	2	0.017	0.017

FIG. 3. Haplotype features in an LD block between SNP-25 and SNP-13 with frequencies. The *numbers 1* and *2* indicate major allele and minor allele, respectively. CONT, Control.

tivity as did the wild-type HIF-1α. The results show consistently higher HIF-1α transcription activity in cells transfected with mutant S582 than with wild-type HIF-1α. However, enhanced transactivation capacity of the S582 HIF-1α mutant was observed with statistical significance only under hypoxic condition ($P = 0.012$) (Fig. 4).

Discussion

The estimated prevalence of diabetes in Japan is 13 million, 90% with T2DM as a result of both environmental and genetic factors. So far, only genetic variants of the Calpain-10 gene (19), PPARγ gene (20), and Kir 6.2 gene (21) have been reported to be related to the occurrence of T2DM in large studies, and genes including angiotensin converting enzyme (ACE), aldose reductase (AR), nitric oxide synthase (NOS), VEGF, and paraoxonase 1 (PON1) *etc.* have been reported to contribute to the development of diabetic retinopathy (22).

We previously compared the expression profile of 1000 mRNAs of rat pancreatic islets with those of rat retina, resulting in the identification of 123 commonly expressed genes. These genes are candidates in both development of T2DM and diabetic retinopathy (23). One of them, VEGF, was reported to be a susceptibility gene for both onset of diabetes and diabetic retinopathy (6, 7), and HIF-1α was reported to induce expression predominantly of VEGF and other important genes involved in glucose metabolism under hypoxic condition, leading us to examine the correlation between HIF-1 and T2DM and retinopathy more closely.

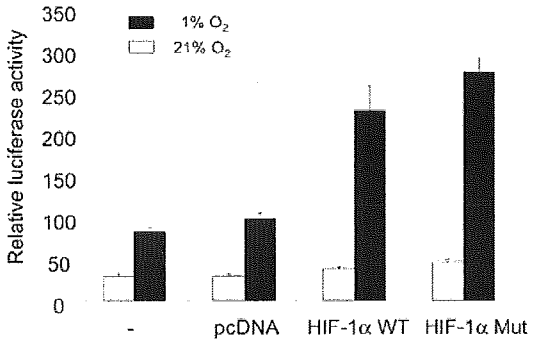

FIG. 4. Transactivation capacity of mutant S582 HIF-1α. Transcription activity with no vector, empty vector, wild type, and P582S HIF-1α (500 ng) was analyzed by cotransfection assay using reporter vector VEGF promoter-pGL3 (200 ng/35-mm well) and a Renilla-luciferase (25 ng/35-mm well) as internal control. The average of three independent experiments is shown (*bar*, ±SD).

In this study, we examined 38 kb covering the entire coding region of the HIF-1α gene in 16 Japanese subjects and identified a total of 35 genetic variations. Thirty-two SNPs were identified in noncoding regions, and three SNPs were identified in coding regions. We defined haplotypes by all possible pairs of 10 SNPs, based on the LD pattern estimated using the frequent SNPs, and examined the associations with T2DM and retinopathy. The haplotype comprising SNP-25 and SNP-13 was most significantly associated with T2DM. cSNP-10 (P582S) was significantly associated with decreased risk of T2DM. Interestingly, the rare allele cSNP-10, resulting in S582, was completely assigned on the 2-2 haplotype comprising SNP-25 and SNP-13, which was observed at significantly higher frequency in control subjects. Thus, the S582 HIF-1α mutant could be protective against the onset of T2DM.

The progress of diabetic retinopathy is known to reflect the duration of diabetes, control of blood glucose level, insulin dosage, and blood pressure. The percentage of patients treated with insulin and hypertension drugs was higher in the group with retinopathy, consistent with previous studies, although the P582S HIF-1α mutation was not associated with onset of diabetic retinopathy even after logistic regression analysis.

The same P582S HIF-1α somatic mutation was found in one of five androgen-independent prostate cancer samples in a recent study, although the mutant was not functionally characterized (24). In addition, an HIF-1α polymorphism, P582S, was identified in a study of renal cell cancers, but the significance in renal cell cancer patients and controls differs in two studies (25, 26). Recently, a P582S HIF-1α mutation was identified in prostate cancer and was reported to enhance transcriptional activity as a result of increased stability under normoxic conditions, resulting in increased tumor microvessel density (27, 28). Proline 582 has not been identified as a site for HIF-1α hydroxylation and is not known to mediate VHL binding. Moreover, the substitution of serine for proline in this position does not appear to prevent VHL binding *in vitro* to a fragment of HIF-1α after hydroxylation at proline 564 (29) Thus, if proline 582 is not a target for hydroxylation, conformational changes induced by the proline to serine substitution could influence hydroxylation at other sites as well as degradation *in vivo*.

HIF-1α is an important inducing factor of VEGF, a key factor in angiogenesis of islets in the pancreatic developmental stage in determining β-cell mass and properties (7), although a high expression level of HIF-1α is observed in hypoxic human adult pancreatic islets and is reported to be correlated with apoptosis (30). In the present study in HEK293 renal cells, the mutant S582 showed a consistently higher level of HIF-1α transcriptional activity than in wild type, and the enhanced transactivation capacity of the mutant was observed with statistical significance only under hypoxic conditions. Accordingly, polymorphism P582S, by enhancing the transcriptional activity of target genes, could be a protective factor against onset of T2DM by its activities in the pancreatic developmental stage. When the two groups with and without S582 are compared, there are no significant differences in

age, BMI, HbA_{1C}, and the presence or absence of insulin therapy (data not shown), partly because of the small number of samples. Functional analysis of the mutant protein S582 HIF-1α using β-cell- or endothelium-derived cell lines might also be required. We did not detect a significant difference in P582S allele frequencies in patients with or without retinopathy, but additional studies with an increased number of patients classified with precise clinical information are required to assess the correlation of this variant with diabetic retinopathy.

It has been reported that acute intensive insulin therapy results in transcriptional activation of VEGF via p38 MAPK, phosphatidylinositol-3-kinase, and HIF-1α, producing paradoxical worsening of diabetic blood-retinal barrier breakdown (31). Thus, more attention should be paid to patients with the P582S HIF-1α mutant allele when they begin treatment with insulin therapy. This polymorphism should be further assessed in larger studies as a risk factor for the development of T2DM and as a biomarker for responses to specific therapies, antiangiogenic therapies in particular.

Acknowledgments

We thank S. Oike, R. Kawakami, Y. Yaginuma, I. Uda, Y. Ibe, and T. Takahashi for assistance.

Received May 5, 2005. Accepted July 18, 2005.

Address all correspondence and requests for reprints to: Yukio Horikawa, M.D., Ph.D., Department of Diabetes and Endocrinology, Gifu University School of Medicine, 1-1 Yanagido, Gifu-city, Gifu 501-1194, Japan. E-mail: yhorikaw@cc.gifu-u.ac.jp.

This study was supported by Grant-in-Aid for Scientific Research and for Scientific Research on Priority Areas (C) Medical Genome Science from the Japanese Ministry of Science, Education, Sports, Culture, and Technology; a Health and Labor Science Research Grant for Research on Human Genome and Tissue Engineering from the Japanese Ministry of Health, Labor, and Welfare; and the Naito Foundation.

References

1. 1997 Report of the Expert Committee on the Diagnosis and Classification of Diabetes Mellitus. Diabetes Care 20:1183–1197
2. **Diabetes Control and Complications Trial Research Group** 1997 Clustering of long-term complications in families with diabetes in the diabetes control and complications trial. Diabetes 46:1829–1839
3. **Rema M, Saravanan G, Deepa R, Mohan V** 2002 Familial clustering of diabetic retinopathy in South Indian type 2 diabetic patients. Diabet Med 19:910–916
4. **Duh E, Aiello LP** 1999 Vascular endothelial growth factor and diabetes: the agonist versus antagonist paradox. Diabetes 48:1899–1906
5. **Aiello LP, Avery RL, Arrigg PG, Keyt BA, Jampel HD, Shah ST, Pasquale LR, Thieme H, Iwamoto MA, Park JE, Nguyen HV, Aiello LM, Ferrara N, King GL** 1994 Vascular endothelial growth factor in ocular fluid of patients with diabetic retinopathy and other retinal disorders. N Engl J Med 331:1480–1487
6. **Awata T, Inoue K, Kurihara S, Ohkubo T, Watanabe M, Inukai K, Inoue I, Katayama S** 2002 A common polymorphism in the 5′-untranslated region of the VEGF gene is associated with diabetic retinopathy in type 2 diabetes. Diabetes 51:1635–1639
7. **Lammert E, Cleaver O, Melton D** 2001 Induction of pancreatic differentiation by signals from blood vessels. Science 294:564–567
8. **Forsythe JA, Jiang BH, Iyer NV, Agani F, Leung SW, Koos RD, Semenza GL** 1996 Activation of vascular endothelial growth factor gene transcription by hypoxia-inducible factor 1. Mol Cell Biol 16:4604–4613
9. **Liu Y, Cox SR, Morita T, Kourembanas S** 1995 Hypoxia regulates vascular endothelial growth factor gene expression in endothelial cells. Circ Res 77:638–643
10. **Wang GL, Semenza GL** 1993 General involvement of hypoxia-inducible factor 1 in transcriptional response to hypoxia. Proc Natl Acad Sci USA 90:4304–4308
11. **Wang GL, Jiang BH, Rue EA, Semenza GL** 1995 Hypoxia-inducible factor 1 is a basic-helix-loop-helix-PAS heterodimer regulated by cellular O_2 tension. Proc Natl Acad Sci USA 92:5510–5514
12. **Maxwell PH, Wiesener MS, Chang GW, Clifford SC, Vaux EC, Cockman ME, Wykoff CC, Pugh CW, Maher ER, Ratcliffe PJ** 1999 The tumor suppressor protein VHL targets hypoxia-inducible factors for oxygen-dependent proteolysis. Nature 399:271–275
13. **Huang LE, Gu J, Schau M, Bunn HF** 1998 Regulation of hypoxia-inducible factor α is mediated by an O_2-dependent degradation domain via the ubiquitin-proteasome pathway. Proc Natl Acad Sci USA 95:7987–7992
14. **Silander K, Scott LJ, Valle TT, Mohlke KL, Stringham HM, Wiles KR, Duren WL, Doheny KF, Pugh EW, Chines P, Narisu N, White PP, Fingerlin TE, Jackson AU, Li C, Ghosh S, Magnuson VL, Colby K, Erdos MR, Hill JE, Hollstein P, Humphreys KM, Kasad RA, Lambert J, Lazaridis KN, Lin G, Morales-Mena A, Patzkowski K, Pfahl C, Porter R, Rha D, Segal L, Suh YD, Tovar J, Unni A, Welch C, Douglas JA, Epstein MP, Hauser ER, Hagopian W, Buchanan TA, Watanabe RM, Bergman RN, Tuomilehto J, Collins FS, Boehnke M; Finland-United States Investigation of NIDDM Genetics (FUSION)** 2004 A large set of Finnish affected sibling pair families with type 2 diabetes suggests susceptibility loci on chromosomes 6, 11, and 14. Diabetes 53:821–829
15. **Iyer NV, Leung SW, Semenza GL** 1998 The human hypoxia-inducible factor 1α gene: *HIF1A* structure and evolutionary conservation. Genomics 52:159–165
16. **Semenza GL** 2000 HIF-1 and human disease: one highly involved factor. Genes Dev 14:1983–1991
17. **Yim S, Choi SM, Choi Y, Lee N, Chung J, Park H** 2003 Insulin and hypoxia share common target genes but not the hypoxia-inducible factor-1α. J Biol Chem 278:38260–38268
18. **Kuzuya T, Nakagawa S, Satoh, J, Kanazawa Y, Iwamoto Y, Kobayashi M, Nanjo K, Sasaki A, Seino Y, Ito C, Shima K, Nonaka K, Kadowaki T** 2002 Report of the committee of the Japan Diabetes Society on the classification and diagnostic criteria of diabetes mellitus. Diabetes Res Clin Pract 55:65–85
19. **Horikawa Y, Oda N, Cox NJ, Li X, Orho-Melander M, Hara M, Hinokio Y, Lindner TH, Mashima H, Schwarz PE, del Bosque-Plata L, Horikawa Y, Oda Y, Yoshiuchi I, Colilla S, Polonsky KS, Wei S, Concannon P, Iwasaki N, Schulze J, Baier LJ, Bogardus C, Groop L, Boerwinkle E, Hanis CL, Bell GI** 2000 Genetic variation in the gene encoding calpain-10 is associated with type 2 diabetes mellitus. Nat Genet 26:163–175
20. **Altshuler D, Hirschhorn JN, Klannemark M, Lindgren CM, Vohl MC, Nemesh J, Lane CR, Schaffner SF, Bolk S, Brewer C, Tuomi T, Gaudet D, Hudson TJ, Daly M, Groop L, Lander ES** 2000 The common PPARγ Pro12Ala polymorphism is associated with decreased risk of type 2 diabetes. Nat Genet 26:76–80
21. **Ioannidis JP, Trikalinos TA, Ntzani EE, Contopoulos-Ioannidis DG** 2003 Genetic associations in large versus small studies: an empirical assessment. Lancet 361:567–571
22. **Frank RN** 2004 Diabetic retinopathy. N Engl J Med 350:48–58
23. **Yamada N, Shihara N, Horikawa Y, Wang H, Takeda J, Kishi S** 2005 Expression profile of 1000 mRNAs from rat retina. Kitakanto Med J 55:5–12
24. **Anastasiadis AG, Ghafar MA, Salomon L, Vacherot F, Benedit P, Chen MW, Shabsigh A, Burchardt M, Chopin DK, Shabsigh R, Buttyan R** 2002 Human hormone-refractory prostate cancers can harbor mutations in the O_2-dependent degradation domain of hypoxia inducible factor-1α (HIF-1α). J Cancer Res Clin Oncol 128:358–362
25. **Clifford SC, Astuti D, Hooper L, Maxwell PH, Ratcliffe PJ, Maher ER** 2001 The PVHL-associated SCF ubiquitin ligase complex: molecular genetic analysis of elongin B and C, Rbx 1 and HIF-1α in renal cell carcinoma. Oncogene 20:5067–5074
26. **Ollerenshaw M, Page T, Hammonds J, Demaine A** 2004 Polymorphisms in the hypoxia inducible factor-1α gene (*HIF1A*) are associated with the renal cell carcinoma phenotype. Cancer Genet Cytogenet 153:122–126
27. **Fu XS, Choi E, Bubley GJ, Balk SP** 2005 Identification of hypoxia-inducible factor-1α (HIF-1α) polymorphism as a mutation in prostate cancer that prevents normoxia-induced degradation. Prostate 63:215–221
28. **Tanimoto K, Yoshiga K, Eguchi H, Kaneyasu M, Ukon K, Kumazaki T, Oue N, Yasui W, Imai K, Nakachi K, Poellinger L, Nishiyama M** 2003 Hypoxia-inducible factor-1α polymorphisms associated with enhanced transactivation capacity, implying clinical significance. Carcinogenesis 24:1779–1783
29. **Percy MJ, Mooney SM, McMullin MF, Flores A, Lappin TR, Lee FS** 2003 A common polymorphism in the oxygen-dependent degradation (ODD) domain of hypoxia inducible factor-1α (HIF-1α) does not impair Pro-564 hydroxylation. Mol Cancer 2:31
30. **Moritz W, Meier F, Stroka DM, Giuliani M, Kugelmeier P, Nett PC, Lehmann R, Candinas D, Gassmann M, Weber M** 2002 Apoptosis in hypoxic human pancreatic islets correlates with HIF-1α expression. FASEB J 16:745–747
31. **Poulaki V, Qin W, Joussen AM, Hurlbut P, Wiegand SJ, Rudge J, Yancopoulos GD, Adamis AP** 2002 Acute intensive insulin therapy exacerbates diabetic blood-retinal barrier breakdown via hypoxia-inducible factor-1α and VEGF. J Clin Invest 109:805–815

Original Article

A Functional Variant in the Human Betacellulin Gene Promoter Is Associated With Type 2 Diabetes

Yoshio Nakano,[1] Hiroto Furuta,[1] Asako Doi,[1] Shohei Matsuno,[1] Takayuki Nakagawa,[1] Hiroko Shimomura,[1] Setsuya Sakagashira,[1] Yukio Horikawa,[2] Masahiro Nishi,[1] Hideyuki Sasaki,[1] Tokio Sanke,[3] and Kishio Nanjo[1]

Betacellulin (BTC) plays an important role in differentiation, growth, and antiapoptosis of pancreatic β-cells. We characterized about 2.3 kb of the 5′-flanking region of human *BTC* gene and identified six polymorphisms (−2159A>G, −1449G>A, −1388C>T, −279C>A, −233G>C, and −226A>G). The G allele in the −226A>G polymorphism was more frequent in type 2 diabetic patients (n = 250) than in nondiabetic subjects (n = 254) (35.6% vs. 27.8%, P = 0.007), and the −2159G, −1449A, and −1388T alleles were in complete linkage disequilibrium with the −226G allele. The frequencies of the −279A and −233C alleles were low (7.0 and 2.0% in diabetic patients), and no significant differences were observed. In the diabetic group, insulin secretion ability, assessed by the serum C-peptide response to intravenous glucagon stimulation, was lower in patients with the −226G allele (G/G, 2.96 ± 0.16 ng/ml; G/A, 3.65 ± 0.18 ng/ml; A/A, 3.99 ± 0.16 ng/ml at 5 min after stimulation; P = 0.008). Furthermore, in vitro functional analyses indicated that both the −226G and the −233C alleles caused an ~50% decrease in the promoter activity, but no effects of the −2159A>G, −1449G>A, −1388C>T, and −279C>A polymorphisms were observed. These results suggest that the −226A/G polymorphism of the *BTC* gene may contribute to the development of diabetes. *Diabetes* 54:3560–3566, 2005

Impaired insulin secretion and insulin resistance are major defects observed in type 2 diabetic patients. When it becomes impossible for pancreatic β-cells to secrete the amount of insulin corresponding to the demand in peripheral tissues, blood glucose levels are elevated in diabetic patients. This insufficient insulin secretion is associated with an insufficient β-cell mass in the pancreatic islet and/or functional defects of the β-cells. Several recent reports have shown the importance of the β-cell mass in the pathophysiology of type 2 diabetes (1–4). Regulation of the β-cell mass appears to involve a balance of β-cell replication, neogenesis (the development of new islets from pancreatic ducts), and apoptosis. Some factors that are associated with the regulation of the β-cell mass have been identified (5), and we hypothesized that functional gene polymorphisms in these factors might be associated with the development of diabetes.

Betacellulin (BTC), a member of the epidermal growth factor (EGF) family, was purified from the conditioned medium of a cell line derived from mouse pancreatic β-cell tumors (6). Its primary translational product was composed of 178 amino acid residues, which contained a signal sequence, transmembrane, and cytoplasmic domains in addition to an EGF-like domain (7). The expression of BTC is predominantly found in the pancreas and in the intestine (8). In particular, BTC is expressed in α-, β-, and duct cells in a normal adult pancreas and in primitive duct cells of the fetal pancreas (9). BTC converts the rat pancreatic acinar cell line (AR42J cells) to insulin-expressing cells together with activin A (10) and has the potential for the growth of a rat insulinoma cell line, INS-1 cells (11). BTC promotes the neogenesis of β-cells and accelerates the improvement of glucose tolerance in mice with diabetes induced by selective alloxan perfusion (12). BTC also improves glucose metabolism by promoting the conversion of intraislet precursor cells to β-cells in streptozotocin-treated mice (13). Furthermore, the activation of the EGF receptor by BTC induces an inhibitory effect on apoptosis (14). These observations suggest that BTC plays an important role in differentiation, growth, and antiapoptosis of the pancreatic β-cells.

We previously screened gene polymorphisms in the protein coding exons of the human *BTC* gene in type 2 diabetic patients (15). The frequencies of polymorphisms identified, however, were similar between the diabetic patients and the control subjects. In this study, to examine the role of polymorphisms in the promoter of the human *BTC* gene, we characterized the 5′-flanking region of the human *BTC* gene and screened gene polymorphisms in the promoter in type 2 diabetic patients.

RESEARCH DESIGN AND METHODS

Characterization of the 5′-flanking region of the human *BTC* gene. To assess the portions of the 5′-flanking region of the human *BTC* gene required for promoter activity, a series of deletions of the region were fused to a luciferase reporter gene. The 5′-flanking regions of the human *BTC* gene spanning −2,330 to 160 bp, −881 to 160 bp, −669 to 160 bp, −350 to 160 bp, and −152 to 160 bp numbered relative to the translation start site, were amplified by PCR using Pfu DNA polymerase (Stratagene, La Jolla, CA), and were subcloned into the *Sma*I site of pGL3-basic firefly luciferase reporter vector (Promega, Madison, WI) in the 5′-3′ orientation. The sequences of constructs were confirmed by bidirectional sequencing. We transiently trans-

From [1]The First Department of Medicine, Wakayama Medical University, Wakayama, Japan; the [2]Department of Diabetes and Endocrinology, Gifu University School of Medicine, Gifu, Japan; and the [3]Department of Clinical Laboratory Medicine, Wakayama Medical University, Wakayama, Japan.

Address correspondence and reprint requests to Hiroto Furuta, MD, PhD, The First Department of Medicine, Wakayama Medical University, 811-1 Kimiidera, Wakayama 641-8509, Japan. E-mail: hfuruta@wakayama-med.ac.jp.

Received for publication 2 June 2005 and accepted in revised form 23 August 2005.

Additional information for this article can be found in an online appendix at http://diabetes.diabetesjournals.org.

BTC, betacellulin; CPR, C-peptide response; EGF, epidermal growth factor.

TABLE 1
Clinical characteristics of the subjects enrolled in the present study

	Nondiabetic subjects	Type 2 diabetic patients
n (male/female)	254 (67/187)	250 (135/115)
Age (years)	75.1 ± 8.0	63.1 ± 11.3
BMI (kg/m^2)	21.8 ± 3.7	23.5 ± 3.2
A1C (%)	5.0 ± 0.4	7.4 ± 1.3
Age at diagnosis (years)	—	45.5 ± 9.4
Mode of treatment (D/OHA/Ins) (%)	—	18.8/40.8/40.4

Data are means ± SD unless otherwise indicated. D, diet; Ins, insulin; OHA, oral hypoglycemic agent.

fected 0.1 μg each of these constructs with 0.01 μg pRL-SV40 vector (renilla luciferase under control of SV40 promoter), as an internal control for transfection efficiency, into βTC3 cells using FuGENE6 transfection reagent (Roche Diagnostics, Mannheim, Germany). The βTC3 cells were seeded into 12-well culture plates and were maintained in Dulbecco's modified Eagle's medium containing 4,500 mg/l glucose, 10% fetal bovine serum, and antibiotics (100 units/ml penicillin G sodium and 100 mg/ml streptomycin sulfate). After 48 h, we collected the cells and measured luciferase activity using Dual-luciferase Reporter Assay System (Promega). The relative luciferase activity for each construct was calculated as a fold increase over the activity for the promoterless control vector (pGL3-basic). The data presented represent the means of three independent transfection experiments per construct.

Screening and genotyping of polymorphisms in the promoter region of the human *BTC* gene. About 2.3 kb of the promoter region was amplified with a PCR and sequenced in DNA samples from 20 Japanese type 2 diabetic patients. PCR was carried out using AmpliTaq Gold polymerase (Applied Biosystems, Foster City, CA). Sequencing was carried out using Big Dye Terminator Cycle Sequencing FS Ready Reaction kit (Applied Biosystems) on an automated DNA capillary sequencer (model 310; Applied Biosystems). Polymorphisms identified in this screening were designated according to their location from the translation start site. Sequence information of the primers and the conditions for PCR-direct sequencing are shown in Supplemental Table 1 in the online appendix (available at http://diabetes.diabetesjournals.org).

Polymorphisms identified were genotyped in 250 Japanese type 2 diabetic patients and 254 nondiabetic subjects using PCR direct sequencing. We calculated linkage disequilibrium coefficients (D′ and Δ^2) using the Graphical Overview of Linkage Disequilibrium program (http://www.sph.umich.edu/csg/abecasis/GOLD). All of the type 2 diabetic patients in this study were recruited from patients attending the outpatient clinic of the Wakayama Medical University Hospital. All patients were evaluated for their insulin secretion ability by the serum C-peptide immunoreactivity response (CPR) to intravenous glucagon stimulation. Because renal function affects serum CPR levels, patients with an elevated serum creatinine level (>1.2 mg/dl) were not included. Diabetes was diagnosed according to the criteria of the World Health Organization, and patients who were glutamic acid decarboxylase antibody positive and/or had started insulin therapy within 3 years of the diagnosis of diabetes were excluded from this study. Nondiabetic subjects were chosen using the following criteria: age of >60 years, HbA_{1c} (A1C) of <5.6%, fasting plasma glucose of <110 mg/dl, and no family history of diabetes. The clinical characteristics of type 2 diabetic patients and nondiabetic subjects are shown in Table 1. All of the participants gave their written informed consent before participating in the study. This study was approved by the ethics committee of the Wakayama Medical University.

Assessment of the insulin secretion ability in type 2 diabetic patients. We assessed the insulin secretion ability in type 2 diabetic patients using their serum CPR response to intravenous glucagon stimulation (16). After an overnight fast, glucagon (1 mg/body) was injected intravenously, and serum CPR levels were measured before (CPR0′) and 5 min after (CPR5′) injection, and then, the increment of CPR for 5 min (ΔG5′) was calculated. The patients treated with drugs were instructed not to take their morning oral hypoglycemic agents or insulin on the day of test.

Functional properties of polymorphisms on the promoter activity of the human *BTC* gene. The −279C>A, −233G>C, and −226A>G gene polymorphisms were introduced into the pGL3-reporter vector containing the 5′-flanking region spanning from −669 to 160 bp using QuikChange site-directed mutagenesis kit (Stratagene) for generating five constructs, pGL3-(−669/160)CGA, pGL3-(−669/160)CGG, pGL3-(−669/160)AGA, pGL3-(−669/160)CCA, and pGL3-(−669/160)CCG. Four gene polymorphisms, −2159A>G, −1449G>A, −1388C>T, and −226A>G, were also introduced into the pGL3-reporter vector containing the 5′-flanking region spanning from −2,330 to 160 bp using the same kit for generating three constructs, pGL3-(−2330/160)AGCA, pGL3-(−2330/160)GATA, and pGL3-(−2330/160)GATG. These constructs were transfected into the βTC3 cells, and the relative luciferase activity for each construct was calculated as described above.

Statistical analysis. Results are presented as means ± SE unless otherwise indicated. The proportion of genotypes or alleles was compared by a χ^2 test. Group differences of continuous variables were compared using an unpaired *t* test or a one-way ANOVA followed by a post hoc analysis with a Fisher's protected least-significant difference test. Categorical variables were compared with a χ^2 test. The data of serum CPR levels were log transformed before analyzing. These analyses were performed with the StatView program for Windows (version 5.01; SAS Institute, Cary, NC). A P value of <0.05 was considered to be statistically significant.

RESULTS

Characterization of the 5′-flanking region of the human *BTC* gene. The relative luciferase activities of the reporter constructs in the βTC3 cells are shown in Fig. 1. The construct containing from −350 to 160 bp demonstrated a fivefold increase in activity compared with the promoterless construct ($P < 0.001$), whereas only background activity was obtained with the construct containing from −152 to 160 bp. Furthermore, a significant increase in activity was observed with the addition of the region between −669 and −350 bp ($P = 0.020$). Conversely, the further addition of the region between −881 and −669 bp attenuated the promoter activity ($P = 0.002$). Finally, the promoter activity of the construct containing the region up to −2,330 bp was significantly higher than that of the construct containing the region up to −669 bp ($P < 0.001$). These data suggest that the basal promoter of the human *BTC* gene is located within the −200-bp region between −350 and −152 bp relative to the translation start site, the positive regulatory elements are located within the regions between −669 and −350 bp and between −2,330 and −881 bp, and the negative regulatory element(s) is located within the region between −881 and −669 bp.

Polymorphisms in the promoter region of the human *BTC* gene. About 2.3 kb of the promoter region was screened in 20 Japanese type 2 diabetic patients, and six polymorphisms were identified. These polymorphisms include a G for A substitution at −2,159 bp (−2159A>G), an A for G substitution at −1,449 bp (−1449G>A), a T for C substitution at −1,388 bp (−1388C>T), an A for C substitution at −279 bp (−279C>A), a C for G substitution at −233 bp (−233G>C), and a G for A substitution at −226 bp (−226A>G). All polymorphisms were numbered relative to the translation start site. The reference single nucleotide polymorphism ID numbers of −2159A>G, −1449G>A, −1388C>T, and −226A>G are rs11733938, rs13121979, rs13101336, and rs2278862, respectively.

We genotyped these polymorphisms in 250 type 2 diabetic patients and 254 nondiabetic subjects. The allelic distributions were in the Hardy-Weinberg equilibrium expectations, and the −2159G, −1449A, −1388T, and −226G alleles were in complete linkage disequilibrium with each other (D′ = 1.00, Δ^2 = 1.00). For the −226A>G polymorphism, the G allele was significantly more frequent in type 2 diabetic patients than in nondiabetic subjects (P = 0.007). The odds ratios (OR) of subjects with the G/G or A/G genotype were 1.90 (95% CI 1.05–3.41, P = 0.031) and 1.49 (1.02–2.16, P = 0.038) compared with those having the A/A genotype, respectively. In the −279C>A and −233G>C polymorphisms, no significant differences were observed

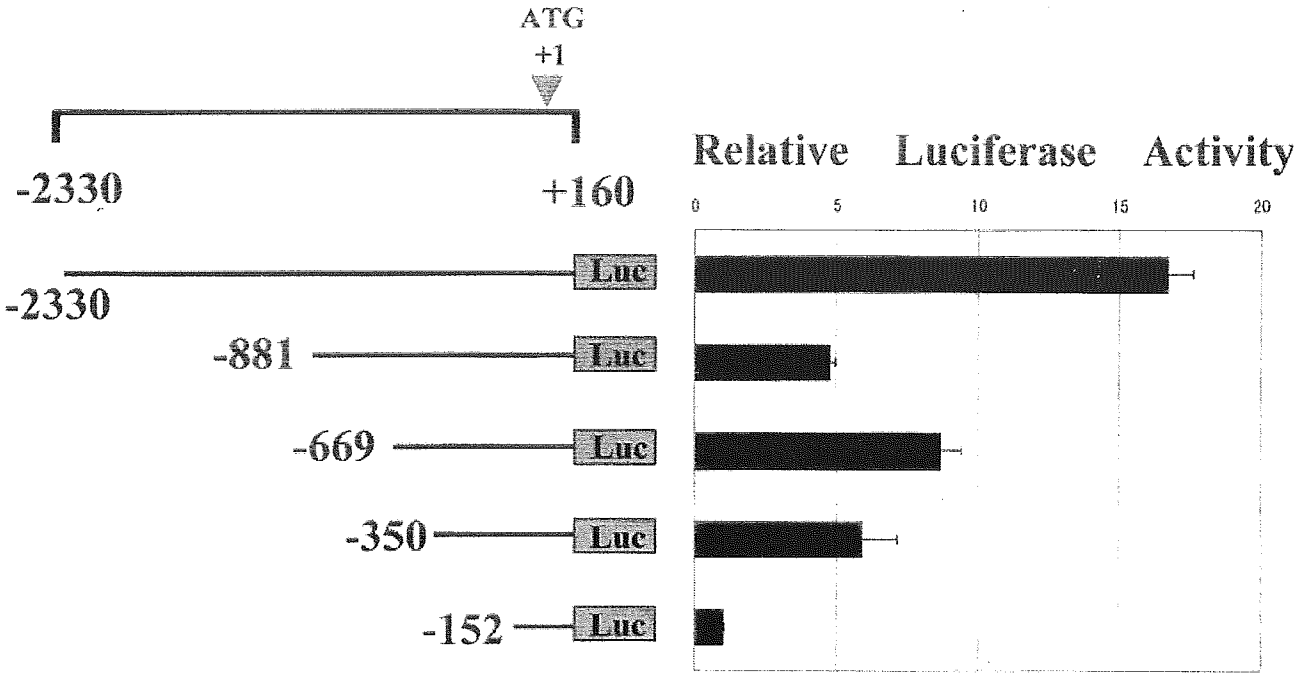

FIG. 1. Deletion analysis of the 5′-flanking region of the human *BTC* gene. The 5′-flanking region was progressively deleted, fused to a firefly luciferase reporter (pGL3-basic) vector, and transfected into βTC3 cells. Cells were cotransfected with a *Renilla* luciferase control (pRL-SV40) vector. The firefly luciferase activity of each construct was normalized in comparison with coexpressed *Renilla* luciferase activity and expressed as the fold increase relative to the activity of the promoterless pGL3-basic vector. All constructs are numbered relative to the translation start site. The data presented represent the means of three independent transfection experiments per construct. Data are means ± SE. The differences in the averaged activities were compared using a one-way ANOVA followed by post hoc test.

in genotypic and allelic distribution between diabetic patients and nondiabetic subjects (Table 2).

Relationship between the −226A>G polymorphism and the insulin secretion ability in type 2 diabetic patients. As shown in Table 3, there were no significant differences in sex, age, age at diagnosis of diabetes, duration of diabetes, maximum BMI, and present BMI among the three groups of type 2 diabetic patients according to the −226A>G genotypes. However, the insulin secretion ability evaluated by the serum CPR response to glucagon stimulation was significantly lower in patients with the G allele (G/G, 2.96 ± 0.16 ng/ml; G/A, 3.65 ± 0.18 ng/ml; and A/A, 3.99 ± 0.16 ng/ml for CPR5′; $P = 0.008$ by ANOVA. G/G, 1.39 ± 0.11 ng/ml; G/A, 1.87 ± 0.11 ng/ml; and A/A, 2.13 ± 0.11 ng/ml for ΔG5′; $P = 0.002$.) (Fig. 2). The fasting serum CPR levels were also lower in patients with the G allele (G/G, 1.58 ± 0.10 ng/ml; G/A, 1.76 ± 0.07 ng/ml; and A/A, 1.86 ± 0.07 ng/ml; $P = 0.182$), and the A1C levels and the percentage of patients with insulin treatment were higher in patients with the G allele, but these differences were not statistically significant.

Effects of polymorphisms on the promoter activity of the human *BTC* gene. To investigate whether the −279C>A, −233G>C, and −226A>G gene polymorphisms would affect the promoter activity of the human *BTC* gene, we constructed four plasmids containing the 5′-flanking region spanning from −669 to 160 bp, pGL3-(−669/160)CGA, pGL3-(−669/160)CGG, pGL3-(−669/160)AGA, and pGL3-(−669/160)CCA vectors. In transient transfection into the βTC3 cells, the pGL3-(−669/160)CGA vector induced luciferase activity sevenfold greater, relative to the promoterless pGL3-basic vector (Fig. 3). On the other hand, the pGL3-(−669/160)CGG vector had an ~50% decrease in the activity compared with the pGL3-(−669/

TABLE 2
Comparison of genotypic and allelic distributions of gene polymorphisms between type 2 diabetic patients and nondiabetic subjects

Polymorphisms	Genotypes				Alleles		
−226A>G	A/A	A/G	G/G		A	G	
Type 2 diabetes	106 (42.4)	110 (44.0)	34 (13.6)	$P = 0.032$	322 (64.4)	178 (35.6)	$P = 0.007$
Nondiabetic	136 (53.5)	95 (37.4)	23 (9.1)		367 (72.2)	141 (27.8)	
−233G>C	G/G	G/C	C/C		G	C	
Type 2 diabetes	240 (96.0)	10 (4.0)	0 (0)	$P = 0.439$	490 (98.0)	10 (2.0)	$P = 0.419$
Nondiabetic	247 (97.2)	7 (2.8)	0 (0)		501 (98.6)	7 (1.4)	
−279C>A	C/C	C/A	A/A		C	A	
Type 2 diabetes	215 (86.0)	35 (14.0)	0 (0)	$P = 0.643$	465 (93.0)	35 (7.0)	$P = 0.655$
Nondiabetic	222 (87.4)	32 (12.6)	0 (0)		476 (93.7)	32 (6.3)	

Data are *n* (%). The results of −2159A>G, −1449G>A, and −1388C>T are not shown because the −2159G, −1449A, and −1388T alleles are in complete linkage disequilibrium with the −226G allele.

TABLE 3
Clinical characteristics and biochemical data of type 2 diabetic patients classified according to their genotypes of the −226A>G polymorphism

	−226A >G genotype			
	G/G	G/A	A/A	*P*
n (male/female)	34 (16/18)	110 (58/52)	106 (61/44)	0.488
Age (years)	62.4 ± 2.0	64.3 ± 1.1	62.2 ± 1.1	0.377
Age at diagnosis (years)	45.6 ± 1.5	45.4 ± 0.9	45.6 ± 1.0	0.976
Duration of diabetes (years)	16.7 ± 1.8	18.6 ± 1.0	16.4 ± 1.0	0.265
Maximum BMI (kg/m^2)	27.0 ± 0.6	26.5 ± 0.3	27.0 ± 0.3	0.554
BMI (kg/m^2)	23.4 ± 0.5	23.3 ± 0.3	23.7 ± 0.3	0.662
A1C (%)	7.7 ± 0.2	7.5 ± 0.1	7.2 ± 0.1	0.072
Mode of treatment (D/OHA/Ins) (*n*)	6/11/17	18/47/45	23/44/39	
Insulin (%)	50.0	40.9	37.7	0.389

Data are shown as means ± SE unless otherwise indicated. *P* values are compared by one-way ANOVA or χ^2 test for existence of insulin treatment. D, diet; Ins, insulin; OHA, oral hypoglycemic agents.

160)CGA vector (3.84 ± 0.23 vs. 6.98 ± 0.33, $P < 0.001$). Furthermore, the pGL3-(−669/160)CCA vector had an ~50% decrease in the activity compared with the pGL3-(−669/160)CGA vector (3.73 ± 0.23 vs. 6.98 ± 0.33, $P < 0.001$). The relative luciferase activity of the pGL3-(−669/160)AGA vector was similar to that of the pGL3-(−669/160)CGA vector (7.30 ± 0.43 vs. 6.98 ± 0.33, $P = 0.533$). Because not only the −226A>G polymorphism but also the −233G>C polymorphism affected the promoter activity of the human *BTC* gene, we further constructed pGL3-(−669/160)CCG vector, but the relative luciferase activity of the pGL3-(−669/160)CCG vector was similar to those of the pGL3-(−669/160)CGG and pGL3-(−669/160)CCA vectors. We next examined the effect of −2159A>G, −1449G>A, and −1388C>T polymorphisms on the promoter activity of the human *BTC* gene, because the −226G allele was in complete linkage disequilibrium with −2159G, −1449A, and −1388T alleles. Four polymorphisms, −2159A>G, −1449G>A, −1388C>T, and −226A>G, were introduced into pGL3-reporter vector containing the 5′-flanking region spanning from −2,330 to 160 bp for generating three plasmids, pGL3-(−2330/160)AGCA, pGL3-(−2330/160)GATA, and pGL3-(−2330/160)GATG. The pGL3-(−2330/160)GATA vector induced luciferase expression ~14-fold greater, relative to the promoterless pGL3-basic vector, and the pGL3-(−2330/160)GATG had an ~50% decrease in activity compared with the pGL3-(−2330/160)GATA vector (14.4 ± 1.20 vs. 8.02 ± 0.50, $P < 0.001$) (Fig. 4). On the other hand, the relative luciferase activity of the pGL3-(−2330/160)GATA vector was similar to that of the pGL3-(−2330/160)AGCA vector (14.4 ± 1.20 vs. 16.4 ± 0.81, $P = 0.131$). These results suggest that −2159A>G, −1449G>A, and −1388C>T polymorphisms do not affect the transcription of the human *BTC* gene.

DISCUSSION

In this study, our purpose was to investigate the role of gene polymorphisms in the promoter of the human *BTC* gene in type 2 diabetic patients. Because the promoter of the human *BTC* gene had not been well studied, we initially characterized about 2.3 kb of the 5′-flanking region of the human *BTC* gene in a pancreatic β-cell line. We then screened gene polymorphisms in this region and found that the G allele of the −226A>G polymorphism was more frequent in type 2 diabetic patients than in nondiabetic subjects. However, the possibility that this

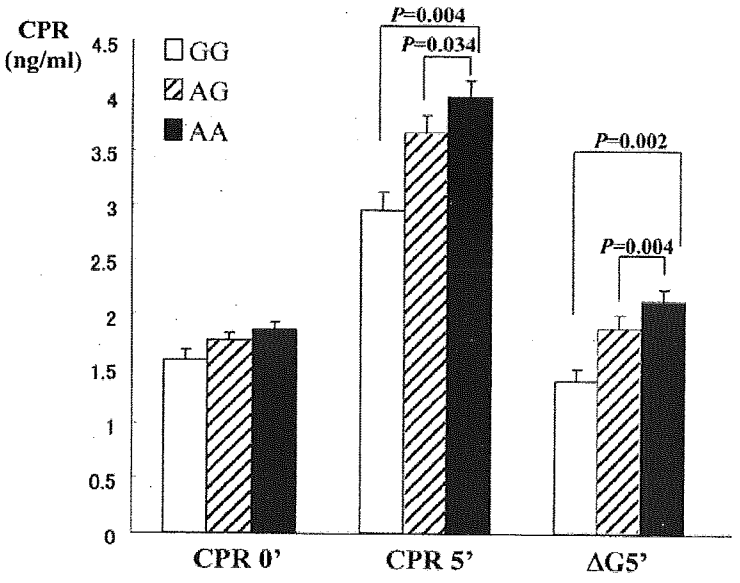

FIG. 2. The effect of the −226A>G polymorphism on fasting C-peptide immunoreactivity (CPR) levels and CPR response to glucagon stimulation in type 2 diabetic patients. The serum CPR levels at 5 min after injection (CPR 5′) and the increment of CPR for 5 min (ΔG5′ = CPR 5′ − CPR 0′) were significantly lower in patients with the G allele. Data are means ± SE. The differences in the averaged CPR levels were compared using a one-way ANOVA followed by post hoc test.

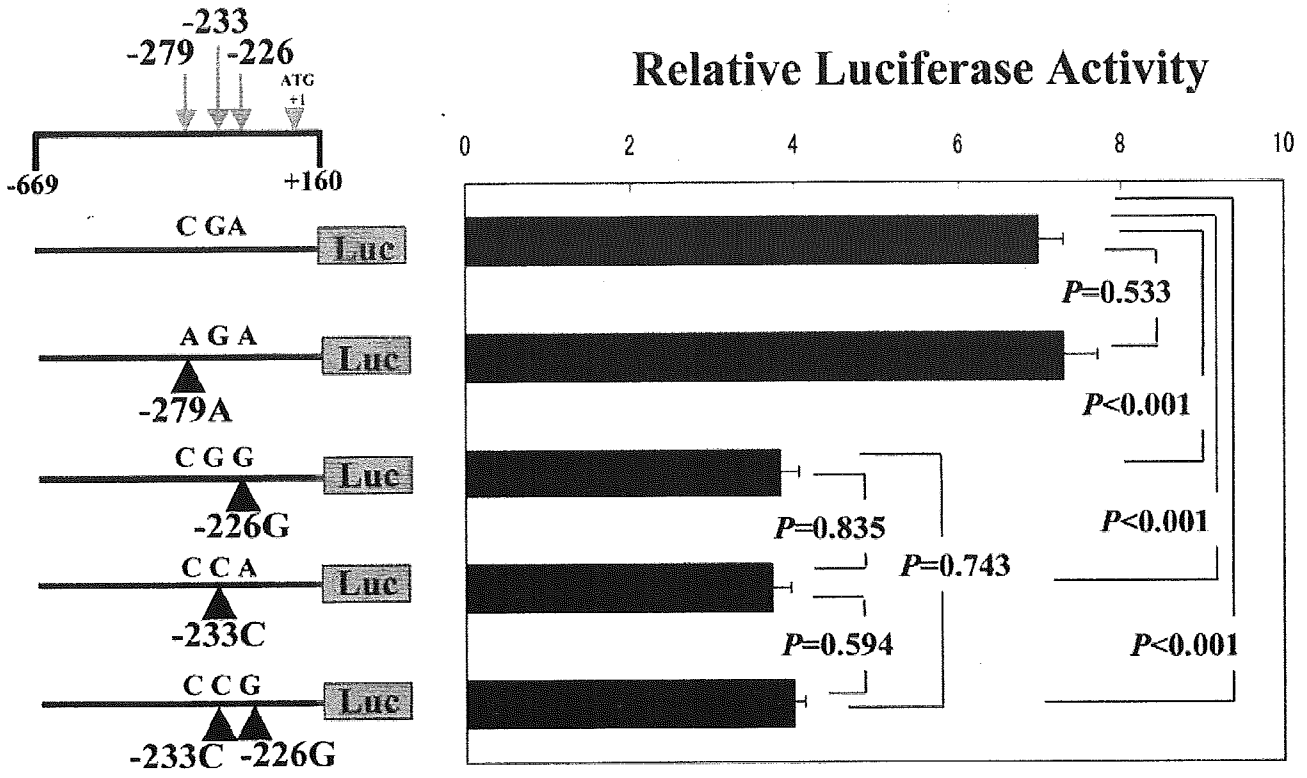

FIG. 3. The effects of the −279C>A, −233G>C, and −226A>G polymorphisms on the promoter activity of the human *BTC* gene. Five plasmids containing the 5′-flanking region, spanning from −669 to 160 bp, with each of five different combinations for the −279C>A, −233G>C, and −226A>G polymorphisms upstream of a luciferase gene transcriptional unit were constructed and transiently transfected into the βTC3 cells. The data presented represent the means of three independent transfection experiments per construct. Data are means ± SE. The differences in the averaged activities were compared using a one-way ANOVA followed by post hoc test.

result is a false-positive finding should be considered, because the sample size of our case-control analysis is small and the *P* values obtained are modest (17). Therefore, we further investigated the effect of the −226A>G polymorphism on clinical profiles of patients and the functional properties of all polymorphisms identified. We first examined the relationship between the G allele of the −226A>G polymorphism and insulin secretion ability in type 2 diabetic patients, because BTC plays an important role in differentiation, growth, and antiapoptosis of the pancreatic β-cells (10–14). Glucagon is a potent stimulus for the pancreatic β-cells, and the serum CPR to intravenous glucagon stimulation has been used to evaluate residual insulin secretion in diabetic patients (16,18). We, therefore, used this test to evaluate the insulin secretion ability in our patient group and observed that the serum CPR to glucagon was significantly lower in patients with the G allele. On the other hand, the A1C level was higher, but not significantly so, in patients with the G allele. The chronic hyperglycemia itself also causes the impairment of β-cell function. However, we think that this may not affect the result, because it has been reported that the serum CPR to glucagon was little influenced by the chronic hyperglycemia (16,19). Moreover, although an influence of oral hypoglycemic agents on the serum CPR should be considered, the percentages of patients treated with oral drugs were almost similar among the groups (G/G, 32%; G/A, 42.7%; A/A, 41.5%; $P = 0.550$). We next examined the functional properties of polymorphisms. A promoter with the −226G allele had an ~50% decrease in the activity. The −226G allele was also in complete linkage disequilibrium with the −2159G, −1449A, and −1338T alleles, but no effects of the −2159A>G, −1449G>A, and −1388C>T polymorphisms on the promoter activity were observed. Furthermore, although we could not observe significant difference in the frequency of −233C allele in our case-control study, a promoter with the −233C allele also had an ~50% decrease in the activity. The −233C allele frequency was only 2.0% in diabetic patients and 1.4% in nondiabetic subjects. The power of our study may be not enough to detect the difference in case-control analysis because of the low frequency of C allele. In subjects with the G/C genotype on the −233G>C polymorphism, 6 of 10 subjects in diabetic group and 2 of 7 subjects in nondiabetic group had the A/G genotype on the −226A>G polymorphism. Subjects with the G/G genotype on the −226A>G polymorphism were not observed in both groups. On the basis of these results, we conclude that a decreased expression of BTC may be associated with the development of type 2 diabetes.

BTC is a member of the EGF family. The addition of BTC promoted proliferation, regeneration, and neogenesis of pancreatic β-cells in both a cell line (11) and diabetic mice developed by treatment with the β-cell toxin (12,13). Furthermore, BTC has an antiapoptotic effect via transactivation of the EGF receptors, and the effect is greater than that by EGF (14). Several reports suggest that a decreased β-cell mass is observed in type 2 diabetic patients (1–4) and plays an important role in the pathogenesis of type 2 diabetes. The β-cell mass is regulated by a balance be-

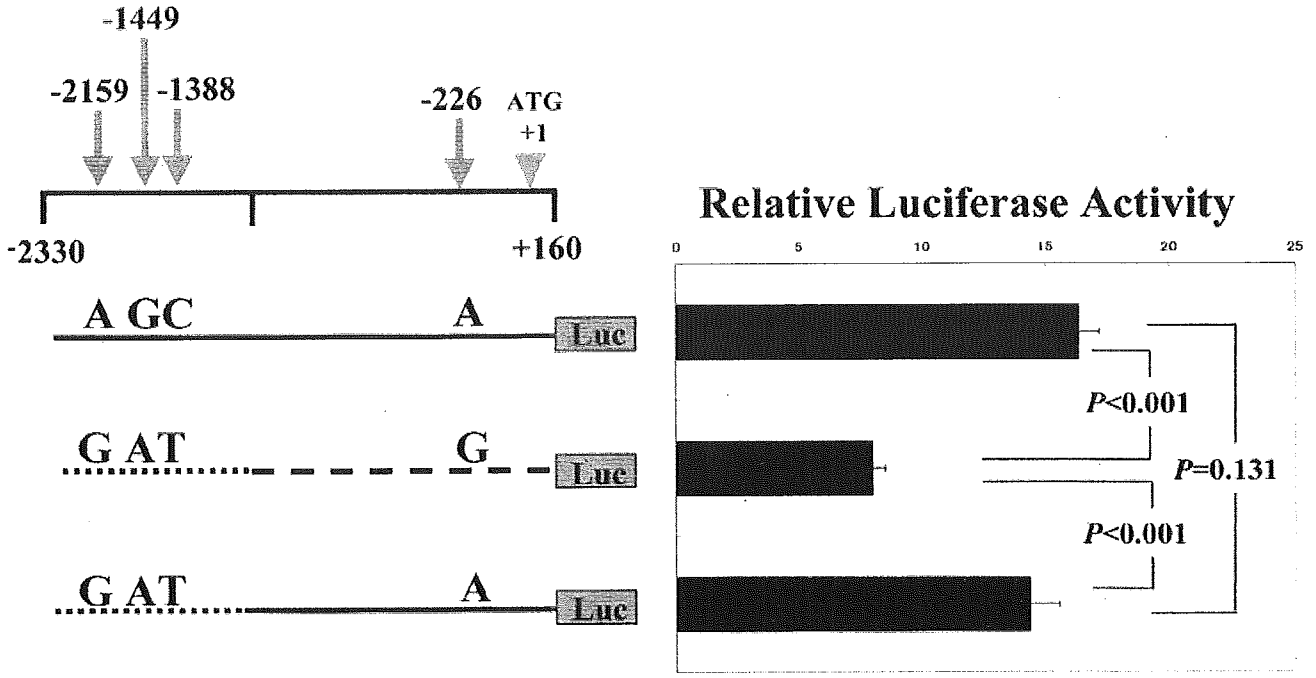

FIG. 4. The effects of the −2159A>G, −1449G>A, and −1388C>T polymorphisms on the promoter activity of the human *BTC* gene. Three plasmids containing the 5′-flanking region, spanning from −2,330 to 160 bp, with each of three different combinations for the −2159A>G, −1449G>A, −1388C>T, and −226A>G polymorphisms upstream of a luciferase gene transcriptional unit were constructed and transiently transfected into the βTC3 cells. No effects of the −2159A>G, −1449G>A, and −1388C>T polymorphisms in the promoter activity were observed. The data presented represent the means of three independent transfection experiments per construct. Data are means ± SE. The differences in the averaged activities were compared using a one-way ANOVA followed by post hoc test.

tween an input (β-cell neogenesis from pancreatic ducts and β-cell replication within islets) and an output (β-cell apoptosis). Because BTC accelerates the input and decelerates the output, a decreased expression of BTC affected by gene polymorphism may accelerate a decrease in β-cell mass in type 2 diabetic patients. *BTC*-null mice have been generated by gene targeting (20). The mice were viable and grew normally. No morphological changes were observed in the newborn pancreases; also, adult $BTC^{+/+}$ and $BTC^{-/-}$ males responded similarly to glucose challenge tests. Their actual data, however, were not shown in the report. In addition to the BTC dysfunction, other genetic and environmental factors, including aging, may be required for the development of overt diabetes.

The sequences surrounding the −226A>G polymorphism were analyzed for potential transcription factor binding sites using TFSEARCH (available at http://www.rwcp.or.jp/papia/). The sequences were similar to the consensus of a caudal-type homeo box (Cdx)-binding site in reverse orientation, and a G for A substitution of the −226A>G polymorphism resulted in disrupting the consensus. Cdx is the family of homeodomain proteins related to the *Drosophila* "caudal" gene, which is required for anterior-posterior regional identity. In the mouse, Cdx1 and Cdx2/3, which are homologs of the *Drosophila* caudal gene, also have functions in anteroposterior patterning and posterior axis elongation (21). In addition, Cdx1 and Cdx2/3 are expressed in the intestine and regulate intestine-specific gene expression (22). The expression of Cdx2/3 is also found in both α- and β-cells (23) and is one of the islet-enriched transcription factors (24). BTC is also predominantly expressed in the endocrine pancreas and intestine (8). This evidence suggests that Cdx protein is a good candidate of the transcription factor, which binds to the region surrounding the −226A>G polymorphism. The −233G>C polymorphism, which is 7 bp upstream from the −226A>G polymorphism, also affected the promoter activity of the *BTC* gene. Because the effects of the −233G>C polymorphism and the −266A>G polymorphisms were not additive, both polymorphisms may affect the binding of an identical transcription factor. The −233G>C polymorphism, however, did not influence the consensus sequence of Cdx binding site on the analysis using TFSEARCH.

It has been recently reported that the Cys7Gly polymorphism in the *BTC* gene is associated with type 2 diabetes in African Americans (25). Our previous study, however, showed that the minor allele frequency was similar between type 2 diabetic patients (1.8%) and nondiabetic subjects (1.8%) in Japanese (15), and the frequency in Japanese patients was lower than in African Americans (32%). Furthermore, no significant difference in the allele frequency between patients and nondiabetic subjects was observed in Caucasians (25). On the other hand, the −226G allele frequency was higher in type 2 diabetic patients than in nondiabetic subjects both in African Americans (25 vs. 20%, $P = 0.14$) and Caucasians (37 vs. 34%, $P = 0.35$) (25), although their differences were not statistically significant. Further studies will be needed to understand the ethnic difference in susceptibility to type 2 diabetes.

ACKNOWLEDGMENTS

This work was supported by a Grant-in-Aid for Scientific Research on Priority Areas "Medical Genome Science" and

by Grant-in-Aid for Scientific Research 13204074 from the Ministry of Education, Culture, Sports, Science and Technology of Japan.

We thank Kanako Fujiuchi for technical assistance.

REFERENCES

1. Butler AE, Janson J, Bonner-Weir S, Ritzel R, Rizza RA, Butler PC: β-Cell deficit and increased β-cell apoptosis in humans with type 2 diabetes. *Diabetes* 52:102–110, 2003
2. Yoon KH, Ko SH, Cho JH, Lee JM, Ahn YB, Song KH, Yoo SJ, Kang MI, Cha BY, Lee KW, Son HY, Kang SK, Kim HS, Lee IK, Bonner-Weir S: Selective beta-cell loss and alpha-cell expansion in patients with type 2 diabetes mellitus in Korea. *J Clin Endocrinol Metab* 88:2300–2308, 2003
3. Sakuraba H, Mizukami H, Yagihashi N, Wada R, Hanyu C, Yagihashi S: Reduced beta-cell mass and expression of oxidative stress-related DNA damage in the islet of Japanese type II diabetic patients. *Diabetologia* 45:85–96, 2002
4. Rhodes CJ: Type 2 diabetes: a matter of beta-cell life and death? *Science* 307:380–384, 2005
5. Nielsen JH, Galsgaard ED, Moldrup A, Friedrichsen BN, Billestrup N, Hansen JA, Lee YC, Carlsson C: Regulation of β-cell mass by hormones and growth factors. *Diabetes* 50 (Suppl. 1):S25–S29, 2001
6. Shing Y, Christofori G, Hanahan D, Ono Y, Sasada R, Igarashi K, Folkman J: Betacellulin: a mitogen from pancreatic beta cell tumors. *Science* 259:1604–1607, 1993
7. Dunbar AJ, Goddard C: Structure-function and biological role of betacellulin. *Int J Biochem Cell Biol* 32:805–815, 2000
8. Seno M, Tada H, Kosaka M, Sasada R, Igarashi K, Shing Y, Folkman J, Ueda M, Yamada H: Human betacellulin, a member of the EGF family dominantly expressed in pancreas and small intestine, is fully active in a monomeric form. *Growth Factors* 13:181–191, 1996
9. Miyagawa J, Hanafusa O, Sasada R, Yamamoto K, Igarashi K, Yamamori K, Seno M, Tada H, Nammo T, Li M, Yamagata K, Nakajima H, Namba M, Kuwajima M, Matsuzawa Y: Immunohistochemical localization of betacellulin, a new member of the EGF family, in normal human pancreas and islet tumor cells. *Endocr J* 46:755–764, 1999
10. Mashima H, Ohnishi H, Wakabayashi K, Mine T, Miyagawa J, Hanafusa T, Seno M, Yamada H, Kojima I: Betacellulin and activin A coordinately convert amylase-secreting pancreatic AR42J cells into insulin-secreting cells. *J Clin Invest* 97:1647–1654, 1996
11. Huotari MA, Palgi J, Otonkoski T: Growth factor-mediated proliferation and differentiation of insulin-producing INS-1 and RINm5F cells: identification of betacellulin as a novel beta-cell mitogen. *Endocrinology* 139: 1494–1499, 1998
12. Yamamoto K, Miyagawa J, Waguri M, Sasada R, Igarashi K, Li M, Nammo T, Moriwaki M, Imagawa A, Yamagata K, Nakajima H, Namba M, Tochino Y, Hanafusa T, Matsuzawa Y: Recombinant human betacellulin promotes the neogenesis of β-cells and ameliorates glucose intolerance in mice with diabetes induced by selective alloxan perfusion. *Diabetes* 49:2021–2027, 2000
13. Li L, Seno M, Yamada H, Kojima I: Betacellulin improves glucose metabolism by promoting conversion of intraislet precursor cells to beta-cells in streptozotocin-treated mice. *Am J Physiol Endocrinol Metab* 285:E577–E583, 2003
14. Saito T, Okada S, Ohshima K, Yamada E, Sato M, Uehara Y, Shimizu H, Pessin JE, Mori M: Differential activation of epidermal growth factor (EGF) receptor downstream signaling pathways by betacellulin and EGF. *Endocrinology* 145:4232–4243, 2004
15. Nakagawa T, Furuta H, Sanke T, Sakagashira S, Shimomura H, Shimajiri Y, Hanabusa T, Nishi M, Sasaki H, Nanjo K: Molecular scanning of the betacellulin gene for mutations in type 2 diabetic patients. *Diabetes Res Clin Pract* 68:188–192, 2005
16. Scheen AJ, Castillo MJ, Lefebvre PJ: Assessment of residual insulin secretion in diabetic patients using the intravenous glucagon stimulatory test: methodological aspects and clinical applications. *Diabetes Metab* 22:397–406, 1996
17. Wacholder S, Chanock S, Garcia-Closas M, El Ghormli L, Rothman N: Assessing the probability that a positive report is false: an approach for molecular epidemiology studies. *J Natl Cancer Inst* 96:434–442, 2004
18. Vague P, Nguyen L: Rationale and methods for the estimation of insulin secretion in a given patient: from research to clinical practice. *Diabetes* 51 (Suppl. 1):S240–S244, 2002
19. Iwasaki Y, Kondo K, Hasegawa H, Oiso Y: C-peptide response to glucagon in type 2 diabetes mellitus: a comparison with oral glucose tolerance test. *Diabetes Res* 25:129–137, 1994
20. Jackson LF, Qiu TH, Sunnarborg SW, Chang A, Zhang C, Patterson C, Lee DC: Defective valvulogenesis in HB-EGF and TACE-null mice is associated with aberrant BMP signaling. *EMBO J* 22:2704–2716, 2003
21. van den Akker E, Forlani S, Chawengsaksophak K, de Graaff W, Beck F, Meyer BI, Deschamps J: Cdx1 and Cdx2 have overlapping functions in anteroposterior patterning and posterior axis elongation. *Development* 129:2181–2193, 2002
22. Walters JR: Cell and molecular biology of the small intestine: new insights into differentiation, growth and repair. *Curr Opin Gastroenterol* 20:70–76, 2004
23. Laser B, Meda P, Constant I, Philippe J: The caudal-related homeodomain protein Cdx-2/3 regulates glucagon gene expression in islet cells. *J Biol Chem* 271:28984–28994, 1996
24. Le Lay J, Matsuoka TA, Henderson E, Stein R: Identification of a novel PDX-1 binding site in the human insulin gene enhancer. *J Biol Chem* 279:22228–22235, 2004
25. Silver K, Tolea M, Wang J, Pollin TI, Yao F, Mitchell BD: The exon 1 Cys7Gly polymorphism within the betacellulin gene is associated with type 2 diabetes in African Americans. *Diabetes* 54:1179–1184, 2005

nature
cell biology

JNK phosphorylation of 14-3-3 proteins regulates nuclear targeting of c-Abl in the apoptotic response to DNA damage

Kiyotsugu Yoshida[1,4], Tomoko Yamaguchi[1], Tohru Natsume[2], Donald Kufe[3] and Yoshio Miki[1,4]

The ubiquitously expressed c-Abl tyrosine kinase localizes to the cytoplasm and nucleus[1,2]. Nuclear c-Abl is activated by diverse genotoxic agents and induces apoptosis[3,4]; however, the mechanisms that are responsible for nuclear targeting of c-Abl remain unclear. Here, we show that cytoplasmic c-Abl is targeted to the nucleus in the DNA damage response. The results show that c-Abl is sequestered into the cytoplasm by binding to 14-3-3 proteins. Phosphorylation of c-Abl on Thr 735 functions as a site for direct binding to 14-3-3 proteins. We also show that, in response to DNA damage, activation of the c-Jun N-terminal kinase (Jnk) induces phosphorylation of 14-3-3 proteins and their release from c-Abl. Together with these results, expression of an unphosphorylated 14-3-3 mutant attenuates DNA-damage-induced nuclear import of c-Abl and apoptosis. These findings indicate that 14-3-3 proteins are pivotal regulators of intracellular c-Abl localization and of the apoptotic response to genotoxic stress.

c-Abl shuttles between the cytoplasm and nucleus by classical mechanisms that involve three nuclear localization signals (NLSs) and one nuclear export signal (NES) in the c-Abl carboxy-terminal region[1,2]. Nuclear c-Abl functions in activating apoptotic signals in the response to DNA damage[3,4]. By contrast, the BCR–ABL fusion protein, which also contains the three NLSs, localizes exclusively in the cytoplasm[5] and confers survival[6]. Forced entrapment of BCR–ABL in the nucleus, however, induces apoptosis[7]. These findings have indicated that the intracellular localization of c-Abl is of importance in dictating whether either survival or apoptosis occurs. The signals that are responsible for targeting c-Abl to the cytoplasm or nucleus are not known.

To investigate partitioning of c-Abl between the cytoplasm and nucleus, we examined subcellular localization of c-Abl before and after genotoxic stress. Treatment of HeLa cells with the DNA-damaging agent adriamycin (ADR), and immunoblot analysis of nuclear and cytoplasmic fractions, showed that c-Abl is targeted to the nucleus (Fig. 1a). As controls, the lysates were reprobed for the nuclear lamin-B and the cytoplasmic IκBα proteins (Fig. 1a). Together with these results, immunostaining of HeLa cells showed nuclear targeting of c-Abl in response to ADR treatment (Fig. 1c). Similar findings were obtained when HeLa cells were treated with other DNA-damaging agents, such as etoposide and ara-C (data not shown). The results also showed that ADR induced nuclear targeting of c-Abl in other cells (see Supplementary Information, Fig. S1a–c). Normal cellular metabolism is associated with the generation of reactive oxygen species (ROS) and c-Abl is activated in the response to oxidative stress[8]. To determine if oxidative stress induces nuclear translocation of c-Abl, cells were treated with hydrogen peroxide as a source of ROS, and nuclear and cytoplasmic lysates were immunoblotted with anti-c-Abl. The results demonstrate that c-Abl is targeted to the nucleus in response to oxidative stress (see Supplementary Information, Fig. S1d). To determine whether nuclear import of c-Abl is transient, cells were analysed during longer periods of ADR exposure. The results indicate that nuclear accumulation of c-Abl is maximal at 2 h and returns to near baseline levels at 8 h (Fig. 1e). In studies with 293T cells expressing Flag-tagged c-Abl (Flag–c-Abl), immunoblot analysis also showed that ADR treatment is associated with localization of c-Abl to the nucleus (Fig. 1b). Immunostaining of the 293T cells confirmed nuclear targeting of Flag–c-Abl in response to ADR (Figs 1d, 3e). Pretreatment with the c-Abl kinase inhibitor, STI571 (ref. 9), had no detectable effect on the ADR-induced nuclear localization of c-Abl (see Supplementary Information, Fig. S1e). Moreover, ADR-induced targeting of a Flag-tagged kinase-inactive c-Abl(K-R)[10] mutant was similar to that of wild-type c-Abl (data not shown), indicating that the c-Abl kinase function is dispensible for nuclear localization. These findings indicate that c-Abl is targeted to the nucleus by a kinase-independent mechanism in the response to DNA damage.

Previous studies have shown that c-Abl-deficient cells are resistant to DNA-damage-induced apoptosis[4] and that activation of nuclear c-Abl is essential for its pro-apoptotic function[10–13]. To determine whether or

[1]Department of Molecular Genetics, Medical Research Institute, Tokyo Medical and Dental University, Tokyo 113-8510, Japan. [2]National Institutes of Advanced Industrial Science and Technology, Biological Information Research Center, 2-41-6 Ohmi, Kohtoh-ku, Tokyo 135-0064, Japan. [3]Dana-Farber Cancer Institute, Harvard Medical School, Boston, MA 02115, USA.
[4]Correspondence should be addressed to K.Y. or Y.M. (e-mail: yos.mgen@mri.tmd.ac.jp or miki.mgen@mri.tmd.ac.jp)

Published online: 6 February 2005, DOI: 10.1038/ncb1228

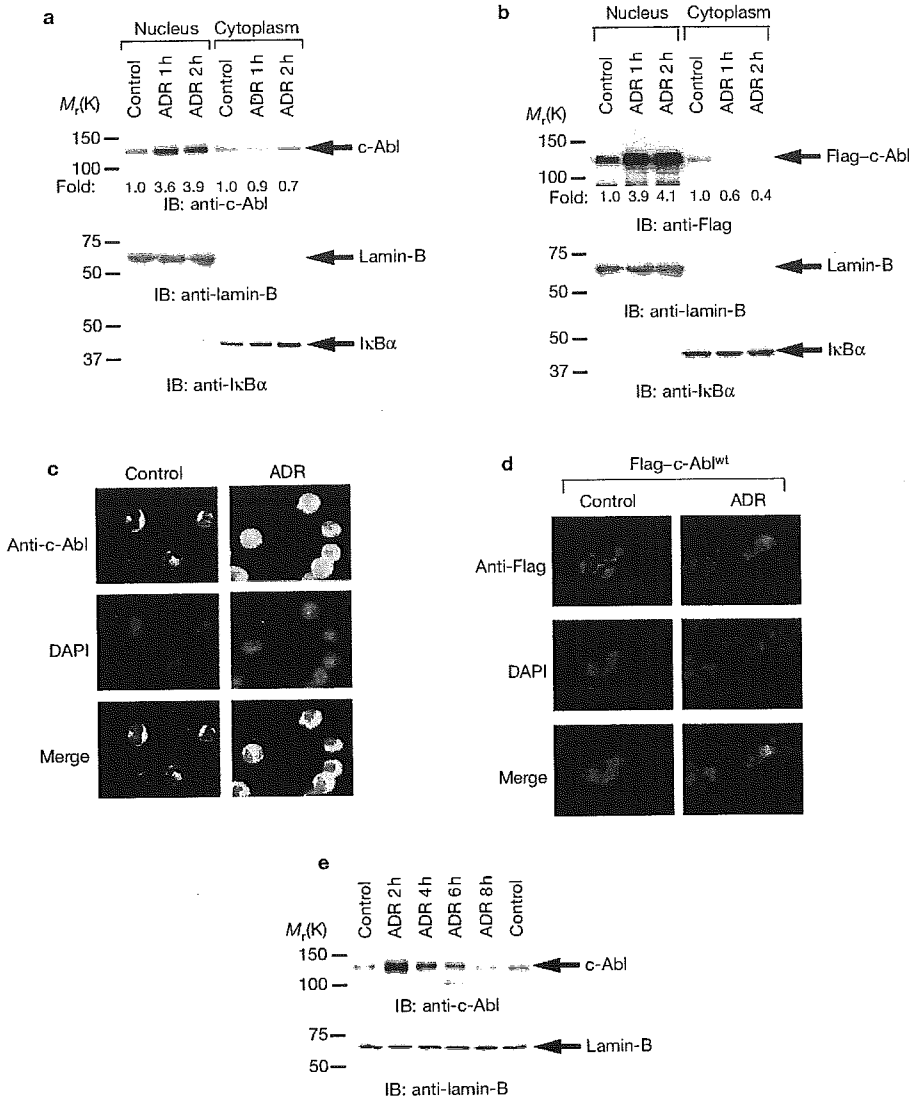

Figure 1 Nuclear translocation of c-ABL in response to DNA damage. (**a**,**b**) HeLa cells (**a**) or 293T cells transfected with Flag–c-ABL (**b**) were left untreated or were treated with adriamycin (ADR). Cell lysates from nuclear and cytoplasmic fractions were subjected to immunoblot (IB) analysis with the indicated antibodies. Protein levels of c-ABL were quantitated by densitometric scanning of the signals. Fold induction was calculated by comparison with the level of nuclear or cytoplasmic c-ABL in control cells. The results are expressed as the mean (standard error, <10%) of at least three independent experiments. (**c**,**d**) HeLa cells (**c**) or 293T cells transfected with Flag–c-ABL (**d**) were left untreated or were treated with ADR for 2 h. After fixation and blocking, cells were incubated with anti- c-ABL (**c**) or anti-Flag (**d**) and counterstained with DAPI (4',6-diamidino-2-phenylindole). Normal mouse immunoglobulin G was used as a negative control (data not shown). (**e**) HeLa cells were treated with ADR for the indicated times. Nuclear lysates were analysed by immunoblotting with anti-c-ABL (upper panel) or anti-lamin-B (lower panel).

not cellular proteins are responsible for subcellular localization of c-Abl, anti-Flag immunoprecipitates from 293T cells expressing Flag–c-Abl were analysed using liquid chromatography, followed by tandem-mass spectrometry[14]. The results indicate that c-Abl associates with 14-3-3 proteins (β, γ, ε, η, σ and ζ). Analysis of anti-14-3-3 immunoprecipitates with anti-c-Abl demonstrated that c-Abl and 14-3-3 proteins form complexes in cells (Fig. 2a). In reciprocal experiments, immunoblot analysis of anti-c-Abl immunoprecipitates with anti-14-3-3 proteins confirmed the association of c-Abl with 14-3-3 proteins (Fig. 2a). When cytoplasmic and nuclear lysates were analysed, the results showed that c-Abl–14-3-3 complexes are localized to the cytoplasm (Fig. 2b). Moreover, treatment with ADR was associated with a marked decrease in these complexes and little, if any, change in localization of 14-3-3 proteins to the cytosol (Fig. 2b,c). Similar results were obtained in response to oxidative stress (see Supplementary Information, Fig. S1d). To determine whether 14-3-3 proteins sequester c-Abl into the cytoplasm, we expressed Flag–c-Abl and green fluorescent protein (GFP) or GFP-14-3-3ζ in 293T cells. Notably, expression of 14-3-3ζ attenuated nuclear localization of c-Abl in control and ADR-treated cells (Fig. 2d). We also knocked-down 14-3-3 proteins by transfection of cells with 14-3-3 small interfering RNAs (siRNAs; Fig. 2e). Downregulation of 14-3-3 proteins was associated with a reduction in cytoplasmic c-Abl

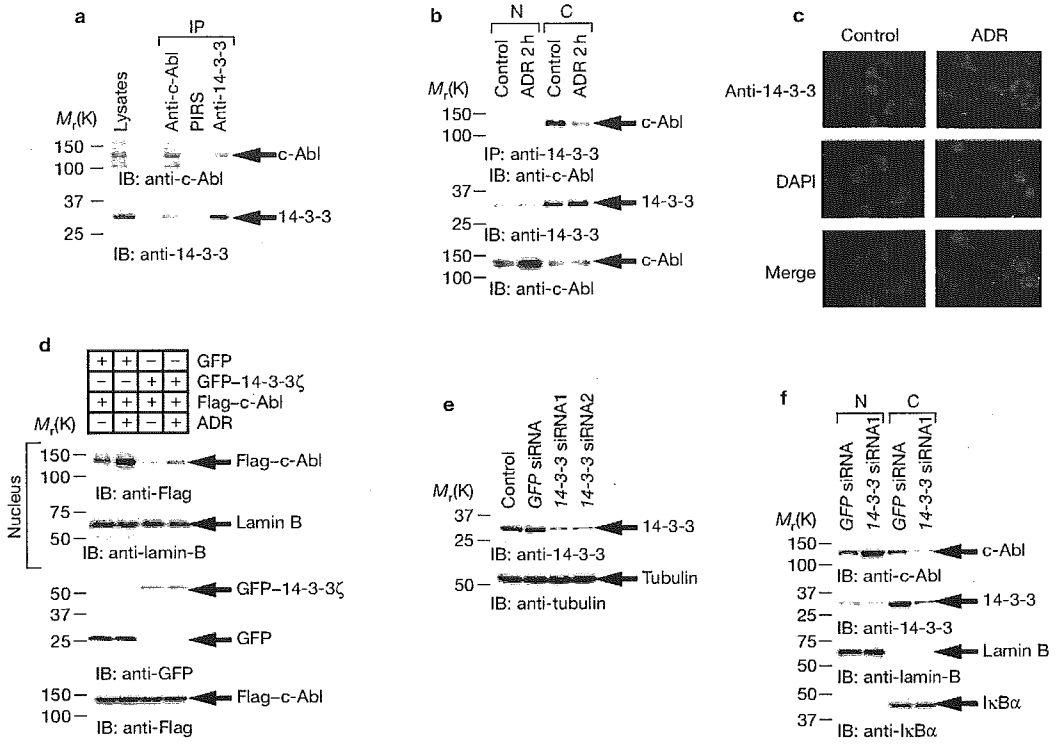

Figure 2 c-ABL interacts with 14-3-3 proteins in the cytoplasm. (**a**) Lysates from HeLa cells were subjected to immunoprecipitation (IP) with pre-immune rabbit serum (PIRS), anti-c-ABL or anti-14-3-3. Cell lysates and immunoprecipitates were analysed by immunoblotting (IB) with anti-c-ABL (upper panel) or anti-14-3-3 (lower panel). (**b**) HeLa cells were treated with adriamycin (ADR) for 2 h. Nuclear (N) and cytoplasmic (C) lysates were subjected to immunoprecipitation with anti-14-3-3 and then immunoblot analysis with anti-c-ABL (upper panel). Lysates were also analysed by immunoblotting with anti-14-3-3 (middle panel) or anti-c-ABL (lower panel). (**c**) HeLa cells were left untreated or were treated with ADR for 2 h. Cells were fixed and stained with anti-14-3-3. Nuclei were stained with DAPI (4',6-diamidino-2-phenylindole). (**d**) 293T cells were transfected with Flag-c-ABL and green fluorescent protein (GFP) vector or GFP–14-3-3ζ. After 2 h treatment with ADR, nuclear lysates were analysed by immunoblotting with anti-Flag (top panel) or anti-lamin-B (second panel). Whole-cell lysates were subjected to immunoblot analysis with anti-GFP (third panel) or anti-Flag (bottom panel). (**e**) HeLa cells were left untransfected (control) or were transfected with GFP small interfering RNA (GFPsiRNA), 14-3-3siRNA1, or 14-3-3siRNA2. Cell lysates were analysed by immunoblotting with anti-14-3-3 (upper panel) or with anti-tubulin (lower panel). (**f**) HeLa cells were transfected with GFPsiRNA or 14-3-3siRNA1. Nuclear and cytoplasmic lysates were subjected to immunoblot analysis with the indicated antibodies.

and an increase in nuclear c-Abl (Fig. 2f). These findings indicate that 14-3-3 proteins sequester c-Abl into the cytoplasm.

14-3-3 proteins bind to a consensus RSXpS/TXP motif and interfere with nuclear import of binding proteins by blocking their NLSs[15,16]. The c-Abl RSVT735LP sequence conforms to the consensus 14-3-3 binding site (Fig. 3a). To determine whether or not c-Abl is phosphorylated on Thr 735, lysates were immunoblotted with an anti-pThr^{735} antibody. Phosphorylation of Thr 735 was detectable in control and ADR-treated cells, indicating that this modification is independent of DNA damage (see Supplementary Information, Fig. S2a). To examine the possibility that phosphorylation of c-Abl on Thr 735 is altered by intracellular translocation of c-Abl in response to DNA damage, nuclear and cytoplasmic lysates were immunoblotted with anti-c-Abl and anti-pThr^{735} antibodies. The findings that the level of c-Abl phosphorylation on Thr 735 parallels that of c-Abl expression in the nucleus and cytoplasm, indicate that this phosphorylation is independent of intracellular c-Abl localization (see Supplementary Information, Fig. S2b). Mutation of c-Abl Thr 735 to Ala abrogated reactivity with anti-pThr^{735} and binding to 14-3-3ζ (Fig. 3b). Binding of c-Abl to 14-3-3σ was also abrogated by the T735A mutation (see Supplementary Information, Fig. S2c). Consistent with these results, c-Abl^{T735A} localized to the nucleus in control and ADR-treated cells (Fig. 3c–e). These findings indicate that 14-3-3 proteins bind to c-Abl at the RSVpTLP motif and thereby sequester c-Abl into the cytoplasm. To further determine if phosphorylation of c-Abl on Thr 735 modulates c-Abl kinase activity, anti-Flag immunoprecipitates of Flag–c-Abl and Flag–c-Abl^{T735A} were analysed for phosphorylation of GST-Crk(120-225) (Fig. 3c). The demonstration that kinase activity of the c-Abl^{T735A} mutant is similar to that of wild-type c-Abl in both control and ADR-treated cells indicates that phosphorylation on Thr 735 is independent of c-Abl kinase activity.

The c-Jun N-terminal kinase (Jnk) protein is activated in the cellular response to DNA damage and phosphorylates 14-3-3ζ on Ser 184 as a mechanism for the release of BAX to mitochondria[17]. To determine whether Jnk regulates the association of c-Abl and 14-3-3 proteins, cells were pretreated with the Jnk inhibitor, SP600125, and then exposed to ADR. Inhibition of Jnk attenuated ADR-induced dissociation of c-Abl from 14-3-3 proteins (Fig. 4a). We also knocked-down MKK7, an upstream activator of Jnk, by transfecting cells with an MMK7 siRNA. As found with SP600125, knocking-down MMK7 attenuated ADR-induced activation of Jnk and release of c-Abl from 14-3-3 proteins (see Supplementary Information, Fig. S3a). Exogenous expression of MMK7, which activates Jnk, was associated with dissociation of c-Abl and 14-3-3

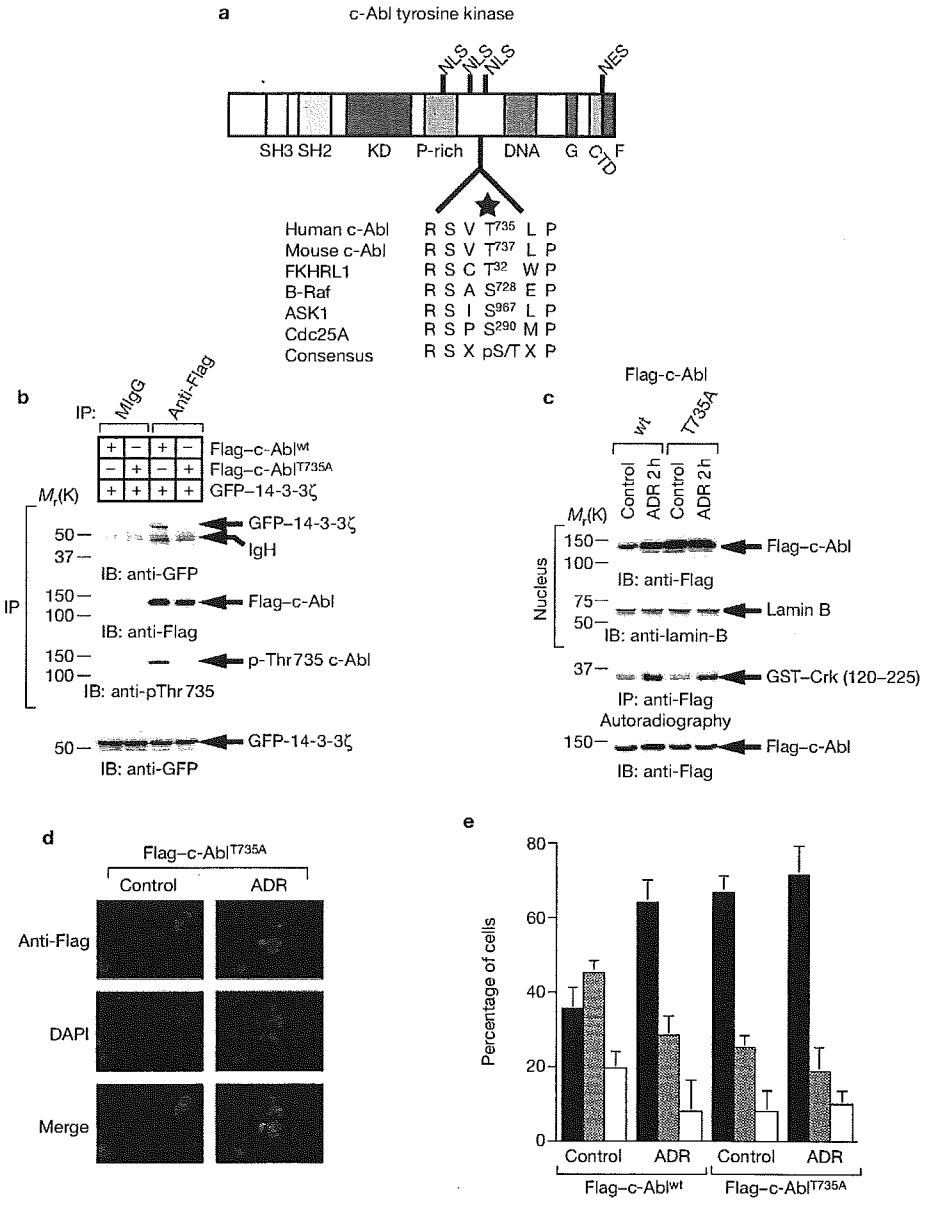

Figure 3 Phosphorylated Thr 735 of c-ABL is the binding site for 14-3-3 proteins. (**a**) Schematic representation of c-ABL tyrosine kinase. SH2, Src homology 2 domain; SH3, Src homology 3 domain; KD, catalytic tyrosine kinase domain; P-rich, proline-rich domain; DNA, DNA-binding domain; G, G-actin binding domain; CTD, RNA polymerase II carboxy-terminal domain binding region; F, F-actin binding domain; NLS, nuclear localization signal; NES, nuclear export signal. The sequence surrounding Thr 735 of c-ABL is shown in enlargement. Similar sequences from other 14-3-3 binding proteins and the consensus 14-3-3 binding motif are also listed. An asterisk marks the threonine/serine that is the putative phosphorylation and 14-3-3 binding site. (**b**) 293T cells were transfected with GFP-14-3-3ζ and Flag-c-ABL wild-type (wt) or T735A variant. Lysates were subjected to immunoprecipitation (IP) with normal mouse immunoglobulin G (MIgG) or anti-Flag, followed by immunoblotting (IB) with the indicated antibodies. Cell lysates were also subjected to immunoblot analysis with anti-GFP (bottom panel). (**c**) 293T cells transfected with Flag-c-ABL wt or T735A mutant were treated with adriamycin (ADR) for 2 h. Nuclear lysates were analysed by immunoblotting with anti-Flag (top panel) or anti-lamin-B (second panel). Anti-Flag immunoprecipitates from whole-cell lysates were incubated with GST-Crk(120-225) and analysed by autoradiography (third panel). Cell lysates were also subjected to immunoblot analysis with anti-Flag (bottom panel). (**d**) 293T cells were transfected with Flag-c-ABL T735A mutant and left untreated or were treated with ADR for 2 h. Fixed cells were stained with anti-Flag and DAPI (4',6-diamidino-2-phenylindole). (**e**) Quantitation of the results in Figs 1d and 3d. The localization of Flag-c-ABL was scored according to whether it was higher in the nucleus (closed bar), evenly distributed between the nucleus and the cytoplasm (dotted bar) or higher in the cytoplasm (open bar). Results are the mean ±SD of values obtained from five fields of 30–100 cells in each of three independent experiments.

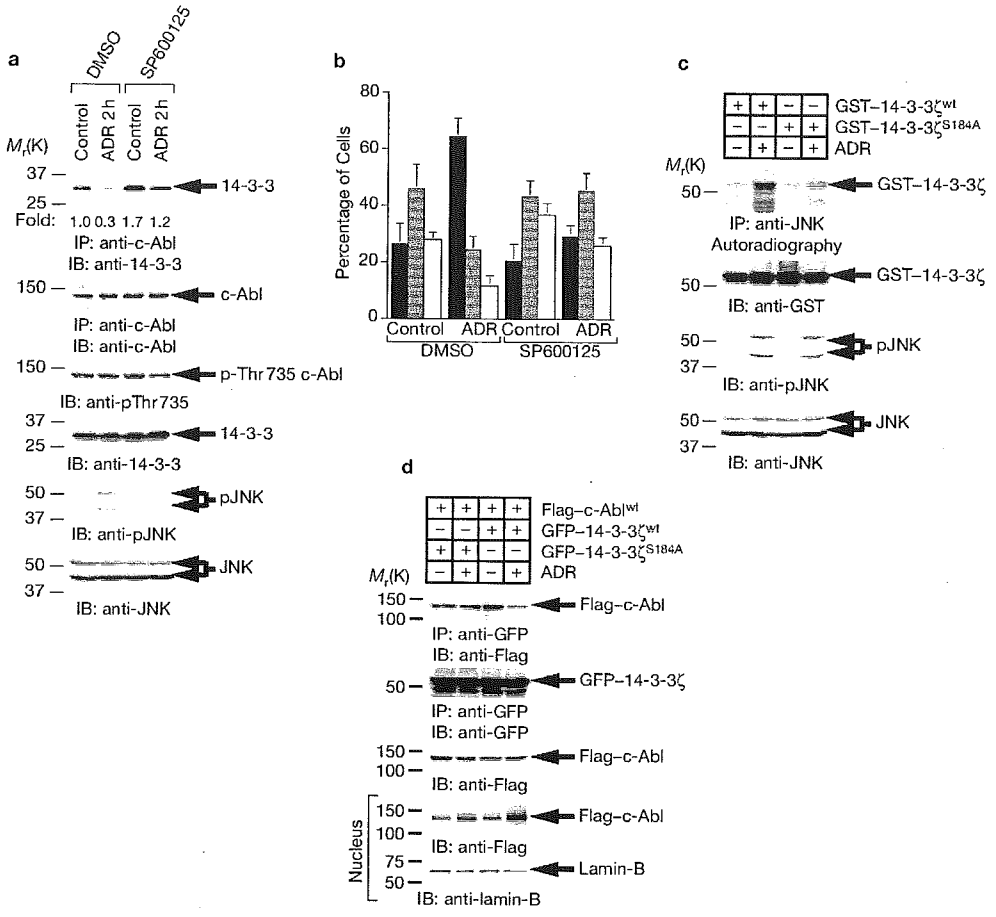

Figure 4 c-Jun N-terminal kinase (JNK) induces release of c-ABL from 14-3-3 proteins in response to DNA damage. (**a**) HeLa cells were treated with dimethyl sulphoxide (DMSO) or SP600125 for 30 min, followed by treatment with adriamycin (ADR). Cell lysates were subjected to immunoprecipitation (IP) with anti-c-ABL and immunoblot (IB) analysis with anti-14-3-3 (top panel) or anti-c-ABL (second panel). Lysates were also analysed by immunoblotting with anti-phospho-c-ABL (Thr 735) (anti-pThr^{735}; third panel), anti-14-3-3 (fourth panel), anti-phospho-JNK (anti-pJNK; fifth panel) or anti-JNK (bottom panel). Protein levels of immunoprecipitated 14-3-3 proteins were quantitated by comparison with the level in control cells. Fold induction was caluculated by comparing to the level in control cells. The results are expressed as the mean (standard error, <10%) of three independent experiments. (**b**) HeLa cells were treated as in **a**. Localization of c-ABL was quantitated as described in the legends to Fig. 3e. (**c**) HeLa cells were left untreated or were treated with ADR for 2 h. Anti-JNK-immunoprecipitates were incubated with glutathione *S*-transferase (GST)-14-3-3ζ wild type (wt) or S184A mutant and [γ-^{32}P]ATP for 15 min at 30 °C. Immunoprecipitation reaction products were resolved by SDS-PAGE and analysed by autoradiography (top panel) or by immunoblotting (IB) with anti-GST (second panel). Cell lysates were subjected to immunoblot analysis with anti-phospho-JNK (anti-pJNK; third panel) or anti-JNK (bottom panel). (**d**) 293T cells were transfected with Flag-c-ABL and GFP-14-3-3ζ wt or S184A mutant. After treatment with ADR for 2 h, whole-cell lysates were subjected to immunoprecipitation (IP) with anti-GFP. The immunoprecipitates were then analysed by immunoblotting with anti-Flag (top panel) or anti-GFP (second panel). Lysates were also subjected to immunoblot analysis with anti-c-ABL (third panel). Nuclear lysates were prepared and analysed by immunoblotting with anti-Flag (fourth panel) or with anti-lamin-B (bottom panel).

proteins (see Supplementary Information, Fig. S3c). Moreover, expression of a dominant-negative MMK7 blocked Jnk activation and release of c-Abl from 14-3-3 proteins (see Supplementary Information, Fig. S3c). It was also shown that downregulation of Jnk attenuated nuclear accumulation of c-Abl following DNA damage (Fig. 4b; also see Supplementary Information, Fig. S3b). To determine whether Jnk phosphorylation of 14-3-3 proteins on Ser 184 releases c-Abl, anti-Jnk immunoprecipitates from cells exposed to ADR were analysed for phosphorylation of 14-3-3ζ or a mutant in which Ser 184 was replaced with Ala (14-3-3ζ^{S184A}). ADR treatment was associated with Jnk phosphorylation of 14-3-3ζ and this response was decreased with the 14-3-3ζ^{S184A} mutant (Fig. 4c). ADR treatment was also associated with dissociation of c-Abl from wild-type 14-3-3ζ and not the 14-3-3ζ^{S184A} mutant (Fig. 4d). Similar findings were obtained in the treatment of cells with hydrogen peroxide (see Supplementary Information, Fig. S3d). These findings support a model in which Jnk phosphorylation of 14-3-3 proteins induces dissociation of the c-Abl–14-3-3 complex and thereby targeting of c-Abl to the nucleus.

To assess the functional significance of the interaction between c-Abl and 14-3-3 proteins, we examined the involvement of 14-3-3 in c-Abl-induced apoptosis. As shown previously[4], expression of c-Abl was associated with induction of apoptosis (Fig. 5a). Moreover, the apoptotic activity of c-Abl was enhanced by ADR treatment (Fig. 5a). By contrast, 14-3-3ζ attenuated c-Abl- and ADR-induced apoptosis

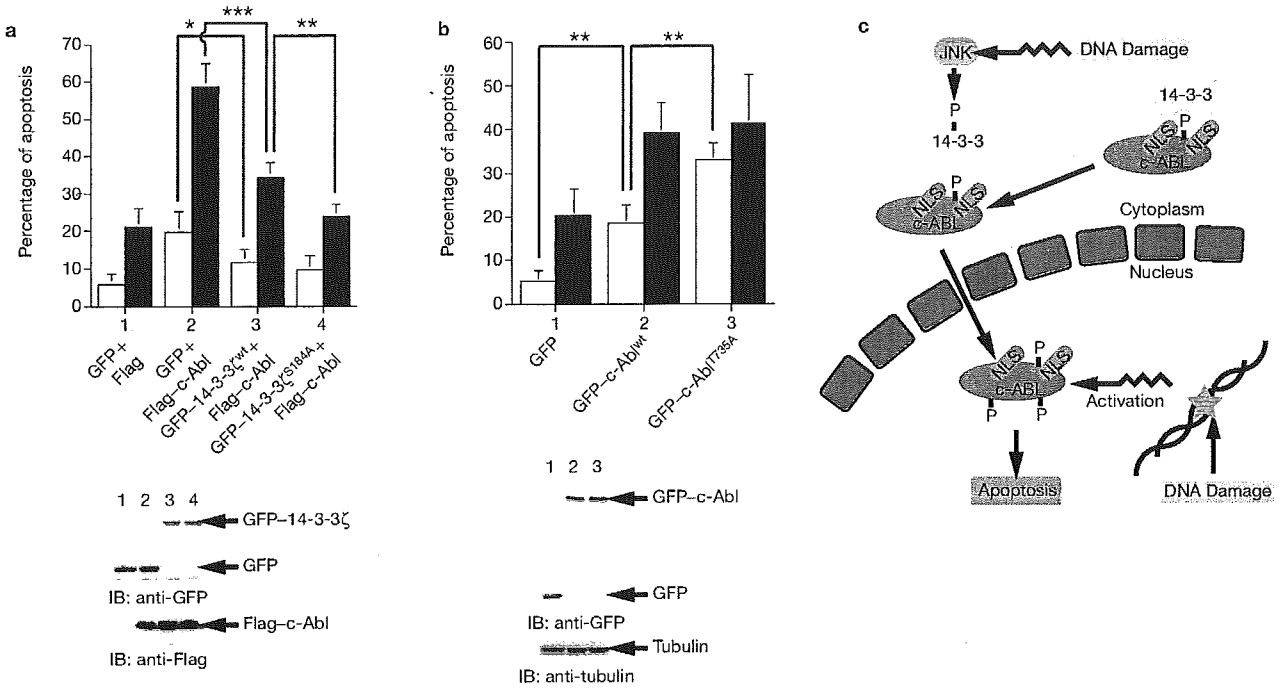

Figure 5 14-3-3 proteins attenuate c-ABL-mediated apoptosis in response to DNA damage. (**a**) 293T cells were transfected with Flag-c-ABL and green fluorescent protein (GFP) vector, GFP–14-3-3ζ wt or S184A mutant. At 24 h post-transfection, cells were left untreated or were treated with adriamycin (ADR) for 24 h. DNA content in cells that were positive for GFP was analysed by FACscan. The results (mean ±SD of eight independent experiments) are represented as the percentage of apoptotic cells with sub-G1 DNA (*P < 0.05, **P < 0.01 and ***P < 0.005). Control cells (open bars); ADR-treated cells (closed bars). Cells were also lysed and analysed by immunoblotting (IB) with anti-GFP (right, upper panel) or anti-Flag (right, lower panel). (**b**) *c-Abl*$^{-/-}$ murine embryonic fibroblasts were transfected with GFP vector, GFP-c-ABL or GFP-c-ABL^{T735A}. At 24 h post-transfection, cells were left untreated or treated with ADR for 24 h. DNA content in cells that were positive for GFP was analysed by FACscan. The results (mean ±SD of three independent experiments) are represented as the percentage of apoptotic cells with sub-G1 DNA (**P < 0.01). Control cells (open bars); ADR-treated cells (closed bars). Cells were also lysed and analysed by immunoblotting with anti-GFP (right, upper panel) or anti-tubulin (right, lower panel). (**c**) A proposed model of the mechanism by which c-ABL translocates to the nucleus in response to DNA damage. Following DNA damage, cytoplasmic sequestration of c-ABL by 14-3-3 proteins is abrogated by c-Jun N-terminal kinase (JNK)-mediated 14-3-3 phosphorylation. Released c-ABL from 14-3-3 proteins then translocates to the nucleus. In the nucleus, c-ABL is activated by DNA damage and induces apoptosis. NLS, nuclear localization signal.

(Fig. 5a). Similar results were obtained in the apoptotic responses to etoposide and ara-C (data not shown). Attenuation of apoptosis was comparable when overexpressing wild-type 14-3-3ζ or the 14-3-3ζ^{S184A} mutant (Fig. 5a); however, following ADR exposure, expression of the 14-3-3ζ^{S184A} mutant conferred a more protective effect on c-Abl-mediated apoptosis (Fig. 5a). Similar results were obtained in the apoptotic response to oxidative stress (see Supplementary Information, Fig. S4a). To determine whether nuclear targeting of c-Abl is associated with induction of apoptosis, we fused various mutants of c-Abl with GFP (see Supplementary Information, Fig. S4b). As previously shown[1,2], the c-Abl NLS deletion mutant (c-AblΔNLS) or NES deletion mutant (c-AblΔNES) localized exclusively in the cytoplasm or the nucleus, respectively (see Supplementary Information, Fig. S4c). Similar patterns of localization were obtained when analysing the cells by fluorescence microscopy (data not shown). Expression of either GFP–c-Abl^{T735A} or GFP–c-AblΔNES was more effective than expression of wild-type c-Abl in inducing apoptosis (see Supplementary Information, Fig. S4d). By contrast, expression of GFP–c-AblΔNLS had little, if any, effect on the induction of apoptosis. Moreover, co-expression of 14-3-3ζ attenuated c-Abl-, but not c-Abl^{T735A}- or c-AblΔNES-induced apoptosis (see Supplementary Information, Fig. S4d). These results support a role for 14-3-3 proteins in inhibiting c-Abl-mediated apoptosis by sequestering c-Abl into the cytoplasm. To directly examine the involvement of 14-3-3 proteins in c-Abl-induced apoptosis, *c-Abl*$^{-/-}$ murine embryonic fibroblasts were transfected with GFP vector, GFP–c-Abl or GFP–c-Abl^{T735A}. Expression of GFP–c-Abl was associated with induction of apoptosis and this effect was enhanced by treatment of cells with ADR (Fig. 5b). Importantly, GFP–c-Abl^{T735A} was more effective than GFP–c-Abl in inducing apoptosis; however, the apoptotic effects of c-Abl and c-Abl^{T735A} were similar when c-Abl was treated with ADR (Fig. 5b). These findings provide support for the involvement of 14-3-3 proteins as negative regulators of apoptosis by cytoplasmic sequestration of c-Abl (Fig. 5c).

The seven isoforms of 14-3-3 have been implicated in regulating apoptosis by sequestering pro-apoptotic proteins, such as BAD, FKHRL1, ASK1, NUR77 and BAX[17–20]. Phosphorylation of the RSXpS/TXP motif on certain 14-3-3 binding proteins is necessary for the interaction with 14-3-3 proteins[21,22]. Other proteins, such as BAX, associate with 14-3-3 proteins by phosphorylation-independent mechanisms[23]. The present results demonstrate that c-Abl binds to 14-3-3 proteins and that this interaction is dependent on phosphorylation of c-Abl on Thr 735 in a conserved RSVTLP motif. Previous work has indicated that 14-3-3 proteins inhibit nuclear import of target proteins by interfering with NLS sites[16]. In this regard, the c-Abl RSVTLP motif resides between the second and third NLSs that are located at amino acids 707–720

and 759–772, respectively (Fig. 3a). The first c-Abl NLS at amino acids 601–615 could also be affected by binding of c-Abl to 14-3-3 proteins. Our results also indicate that Thr 735 phosphorylation is constitutive and not regulated by exposure to DNA-damaging agents. The kinase that is responsible for phosphorylation of c-Abl on Thr 735 is, at present, not known. Importantly, however, expression of c-Abl with a T735A mutation disrupted binding to 14-3-3 proteins and resulted in targeting of c-Abl to the nucleus. These findings indicate that nuclear import of c-Abl is regulated by binding to 14-3-3 proteins in the cytoplasm.

Post-translational modifications of 14-3-3 proteins have been shown to modulate their binding affinity to target proteins[24]. Moreover, recent work has shown that Jnk-mediated phosphorylation of 14-3-3 proteins induces their release from BAX[17]. The present studies demonstrate that Jnk phosphorylation of 14-3-3 proteins induces their release from c-Abl. Jnk has been shown to phosphorylate 14-3-3ζ on Ser 184 (ref. 17). In this context, expression of a Jnk phosphorylation site 14-3-3ζ^{S184A} mutant attenuated DNA-damage-induced localization of c-Abl in the nucleus. These findings collectively support a model in which Jnk phosphorylates 14-3-3 proteins and releases cytoplasmic pools of c-Abl for import into the nucleus and thereby amplification of the apoptotic response (Fig. 5c). Together with this model, the c-Abl kinase function was dispensible for release of c-Abl from 14-3-3 proteins and for import of c-Abl into the nucleus. Previous studies show that, following apoptotic stimuli, 14-3-3 proteins are cleaved by caspases at the C-terminal region, resulting in release of BAD or BAX to the mitochondrial membrane[23,25]. Although this model represents another potential mechanism for dissociation of c-Abl from 14-3-3 proteins, only two isomers of 14-3-3 — ε and θ — are reported to be caspase substrates[23,25]. Moreover, caspase activation occurs in relatively later periods following DNA damage. Given the present findings that nuclear targeting of c-Abl is prompt and transient, it is conceivable that Jnk phosphorylation of 14-3-3 proteins is an initial step for the release of c-Abl. Our results also show that expression of the 14-3-3ζ^{S184A} mutant attenuates c-Abl-mediated apoptosis in the DNA-damage response. Sequestration of c-Abl into the cytoplasm by binding to 14-3-3 proteins therefore represents a potential mechanism by which cells modulate the apoptotic response to genotoxic stress.

METHODS

Cell culture. Human HeLa, 293T embryonal kidney and MCF-7 breast carcinoma cells (ATCC) and murine embryonic fibroblasts[10] were cultured in Dulbecco's modified Eagle's medium (DMEM) supplemented with 10% heat-inactivated fetal bovine serum (FBS), 100 units/ml penicillin, 100 μg ml^{-1} streptomycin and 2 mM L-glutamine. Human U-937 and HL-60 myeloid leukaemia cells (ATCC) were grown in RPMI 1640 medium containing 10% FBS, antibiotics and L-glutamine. Cells were treated with 1 μM ADR (Sigma-Aldrich, St Louis, MO), 10 μM etoposide (Sigma-Aldrich), 10 μM ara-C (Sigma-Aldrich), hydrogen peroxide (Nakalai Tesque, Kyoto, Japan) or 10 μM SP600125 (Calbiochem-Novabiochem, San Diego, CA).

Plasmids. 14-3-3ζ and 14-3-3σ cDNAs were isolated by reverse transcription PCR (RT-PCR) from HeLa cells and cloned into pGFP-C1 (BD Clontech, Palo Alto, CA) and pGEX4T1 (Amersham Biosciences, Piscataway, NJ). Site-directed mutagenesis was performed and the mutation was confirmed by DNA sequencing. c-Abl wild-type and c-Abl (K-R) cDNAs were prepared as described elsewhere[4]. Glutathione *S*-transferase (GST)-tagged Jnk and MKK7 were also prepared as described previously[26].

Cell transfections. Cell transfections were performed as described previously[4,10]. The total DNA concentration was kept constant by including an empty vector.

Protein identification by LC-MS/MS analysis. Flag–c-Abl-associated complexes were digested with Lys-C, and the resulting peptides were analysed using a nanoscale liquid chromatography-mass spectrometry (MS)/MS system as described previously[14].

Immunoprecipitation and immunoblot analysis. Cell lysates were prepared[26] and cleared by centrifugation at 12,000 *g* for 15 min. Soluble proteins were incubated with anti-Flag (Sigma-Aldrich), anti-GFP (Nakalai Tesque), anti-c-Abl (Santa Cruz Biotechnology, Santa Cruz, CA), anti-14-3-3 protein (Upstate, Charlottesville, VA) or anti-Jnk (Santa Cruz Biotechnology) antibodies for 2 h at 4 °C followed by a 1 h incubation with protein A- (Amersham Biosciences) or G- (Zymed Laboratories, South San Francisco, CA) Sepharose beads. The immune complexes were washed three times with lysis buffer. Cell lysates or immunoprecipitates were separated by SDS-PAGE and transferred to nitrocellulose filters. The filters were then incubated with anti-Flag, anti-GFP, anti-c-Abl (Calbiochem-Novabiochem), anti-phospho-c-Abl (Thr 735) (Cell Signaling Technology, Beverly, MA), anti-14-3-3 (Santa Cruz Biotechnology), anti-Jnk, anti-phospho-Jnk (Cell Signaling Technology), anti-MKK7 (Santa Cruz Biotechnology), anti-GST (Nakalai Tesque) or anti-tubulin (Sigma-Aldrich). The antigen–antibody complexes were visualized using chemiluminescence (PerkinElmer, Wellesley, MA).

Subcellular fractionation. Subcellular fractionation was performed as described previously[27]. Purity of the fractions was monitored by immunoblot analysis with anti-lamin-B (Calbiochem-Novabiochem) and anti-IκBα (Santa Cruz Biotechnology).

Immunofluorescence assays. Cells were cultured in 4-well chamber slides. After washing once with phosphate-buffered saline (PBS), cells were fixed in 3.2% paraformaldehyde and permeabilized in 0.5% Triton X-100 in PBS for 10 min. Fixed cells were washed twice in PBS and blocked with 5% goat serum in PBS for 1 h. After washing with PBS three times, cells were incubated with anti-Flag, anti-c-Abl (BD PharMingen, San Diego, CA) or anti-14-3-3 protein for 3 h. Immune complexes were then stained with goat anti-mouse immunoglobulin G conjugated with fluorescein (FITC) or rhodamine (TRITC) antibodies (Sigma-Aldrich). Stained cells were mounted with Vectashield Mounting Medium with 4′,6-diamidino-2-phenylindole (DAPI; Vector Laboratories, Burlingame, CA) and analysed with a Nikon Eclipse TE2000-U microscope.

siRNA transfections. Small interfering RNAs (siRNAs) were synthesized and purified by Qiagen (Valencia, CA). The siRNA sequence for targeting MKK7 was described elsewhere[28]. GFP siRNA were used as a negative control[27]. 14-3-3 protein siRNAs were purchased from Santa Cruz Biotechnology. Transfection of siRNAs was performed in the presence of oligofectamine (Invitrogen, Carlsbad, CA).

***In vitro* kinase assays.** *In vitro* kinase assays were performed as described previously, using GST-Crk(120-225) or GST-14-3-3ζ as a substrate[26].

Assessment of apoptosis. DNA content was assessed by staining ethanol-fixed cells with propidium iodide and monitoring by FACScan (Becton Dickinson, San Jose, CA). The numbers of cells that were positive for green fluorescence with sub-G_1 DNA content were determined using the CellQuest program (Becton Dickinson).

BIND identifiers. Four BIND identifiers (www.bind.ca) are associated with this manuscript: 199701, 199702, 199703 and 199704.

Note: Supplementary Information is available on the Nature Cell Biology website.

ACKNOWLEDGEMENTS

This work was supported by grants from the Ministry of Education, Science and Culture of Japan (K.Y. and Y.M.), the Mitsubishi Pharma Research Foundation (K.Y.), the Tokyo Biochemical Research Foundation (K.Y.), Uehara Memorial Foundation (K.Y.) and also by grants CA29431 and CA98628 from the National Cancer Institute (D.K.).

COMPETING FINANCIAL INTERESTS

The authors declare that they have no competing financial interests.

Received 10 November 2004; accepted 17 December 2004
Published online at http://www.nature.com/naturecellbiology.

1. Wen, S. T., Jackson, P. K. & Van Etten, R. A. The cytostatic function of c-Abl is controlled by multiple nuclear localization signals and requires the p53 and Rb tumor suppressor gene products. *EMBO J.* **15**, 1583–1595 (1996).
2. Taagepera, S. *et al.* Nuclear-cytoplasmic shuttling of c-ABL tyrosine kinase. *Proc. Natl Acad. Sci. USA* **95**, 7457–7462 (1998).
3. Kharbanda, S. *et al.* Activation of the c-Abl tyrosine kinase in the stress response to DNA-damaging agents. *Nature* **376**, 785–788 (1995).
4. Yuan, Z. M. *et al.* Regulation of DNA damage-induced apoptosis by the c-Abl tyrosine kinase. *Proc. Natl Acad. Sci. USA* **94**, 1437–1440 (1997).
5. Wetzler, M. *et al.* Subcellular localization of Bcr, Abl, and Bcr-Abl proteins in normal and leukemic cells and correlation of expression with myeloid differentiation. *J. Clin. Invest.* **92**, 1925–1939 (1993).
6. Raitano, A. B., Whang, Y. E. & Sawyers, C. L. Signal transduction by wild-type and leukemogenic Abl proteins. *Biochim. Biophys. Acta* **1333**, F201–F216 (1997).
7. Vigneri, P. & Wang, J. Y. Induction of apoptosis in chronic myelogenous leukemia cells through nuclear entrapment of BCR–ABL tyrosine kinase. *Nature Med.* **7**, 228–234 (2001).
8. Sun, X., Wu, F., Datta, R., Kharbanda, S. & Kufe, D. Interaction between protein kinase C delta and the c-Abl tyrosine kinase in the cellular response to oxidative stress. *J. Biol. Chem.* **275**, 7470–7473 (2000).
9. Druker, B. J. *et al.* Effects of a selective inhibitor of the Abl tyrosine kinase on the growth of Bcr–Abl positive cells. *Nature Med.* **2**, 561–566 (1996).
10. Yoshida, K., Komatsu, K., Wang, H. G. & Kufe, D. c-Abl tyrosine kinase regulates the human Rad9 checkpoint protein in response to DNA damage. *Mol. Cell. Biol.* **22**, 3292–3300 (2002).
11. Gong, J. G. *et al.* The tyrosine kinase c-Abl regulates p73 in apoptotic response to cisplatin-induced DNA damage. *Nature* **399**, 806–809 (1999).
12. Agami, R., Blandino, G., Oren, M. & Shaul, Y. Interaction of c-Abl and p73α and their collaboration to induce apoptosis. *Nature* **399**, 809–813 (1999).
13. Yuan, Z. M. *et al.* p73 is regulated by tyrosine kinase c-Abl in the apoptotic response to DNA damage. *Nature* **399**, 814–817 (1999).
14. Natsume, T. *et al.* A direct nanoflow liquid chromatography-tandem mass spectrometry system for interaction proteomics. *Anal. Chem.* **74**, 4725–4733 (2002).
15. Tzivion, G. & Avruch, J. 14-3-3 proteins: active cofactors in cellular regulation by serine/threonine phosphorylation. *J. Biol. Chem.* **277**, 3061–3064 (2002).
16. Muslin, A. J. & Xing, H. 14-3-3 proteins: regulation of subcellular localization by molecular interference. *Cell Signal.* **12**, 703–709 (2000).
17. Tsuruta, F. *et al.* JNK promotes Bax translocation to mitochondria through phosphorylation of 14-3-3 proteins. *EMBO J.* **23**, 1889–1899 (2004).
18. Zha, J., Harada, H., Yang, E., Jockel, J. & Korsmeyer, S. J. Serine phosphorylation of death agonist BAD in response to survival factor results in binding to 14-3-3 not BCL-X(L). *Cell* **87**, 619–628 (1996).
19. Zhang, L., Chen, J. & Fu, H. Suppression of apoptosis signal-regulating kinase 1-induced cell death by 14-3-3 proteins. *Proc. Natl Acad. Sci. USA* **96**, 8511–8515 (1999).
20. Masuyama, N. *et al.* Akt inhibits the orphan nuclear receptor Nur77 and T-cell apoptosis. *J. Biol. Chem.* **276**, 32799–32805 (2001).
21. Muslin, A. J., Tanner, J. W., Allen, P. M. & Shaw, A. S. Interaction of 14-3-3 with signaling proteins is mediated by the recognition of phosphoserine. *Cell* **84**, 889–897 (1996).
22. Yaffe, M. B. *et al.* The structural basis for 14-3-3:phosphopeptide binding specificity. *Cell* **91**, 961–971 (1997).
23. Nomura, M. *et al.* 14-3-3 interacts directly with and negatively regulates pro-apoptotic Bax. *J. Biol. Chem.* **278**, 2058–2065 (2003).
24. Aitken, A. *et al.* Specificity of 14-3-3 isoform dimer interactions and phosphorylation. *Biochem. Soc. Trans.* **30**, 351–360 (2002).
25. Won, J. *et al.* Cleavage of 14-3-3 protein by caspase-3 facilitates bad interaction with Bcl-x(L) during apoptosis. *J. Biol. Chem.* **278**, 19347–19351 (2003).
26. Yoshida, K., Weichselbaum, R., Kharbanda, S. & Kufe, D. Role for Lyn tyrosine kinase as a regulator of stress-activated protein kinase activity in response to DNA damage. *Mol. Cell. Biol.* **20**, 5370–5380 (2000).
27. Yoshida, K., Wang, H. G., Miki, Y. & Kufe, D. Protein kinase Cδ is responsible for constitutive and DNA damage-induced phosphorylation of Rad9. *EMBO J.* **22**, 1431–1441 (2003).
28. Deng, Y., Ren, X., Yang, L., Lin, Y. & Wu, X. A JNK-dependent pathway is required for TNFα-induced apoptosis. *Cell* **115**, 61–70 (2003).

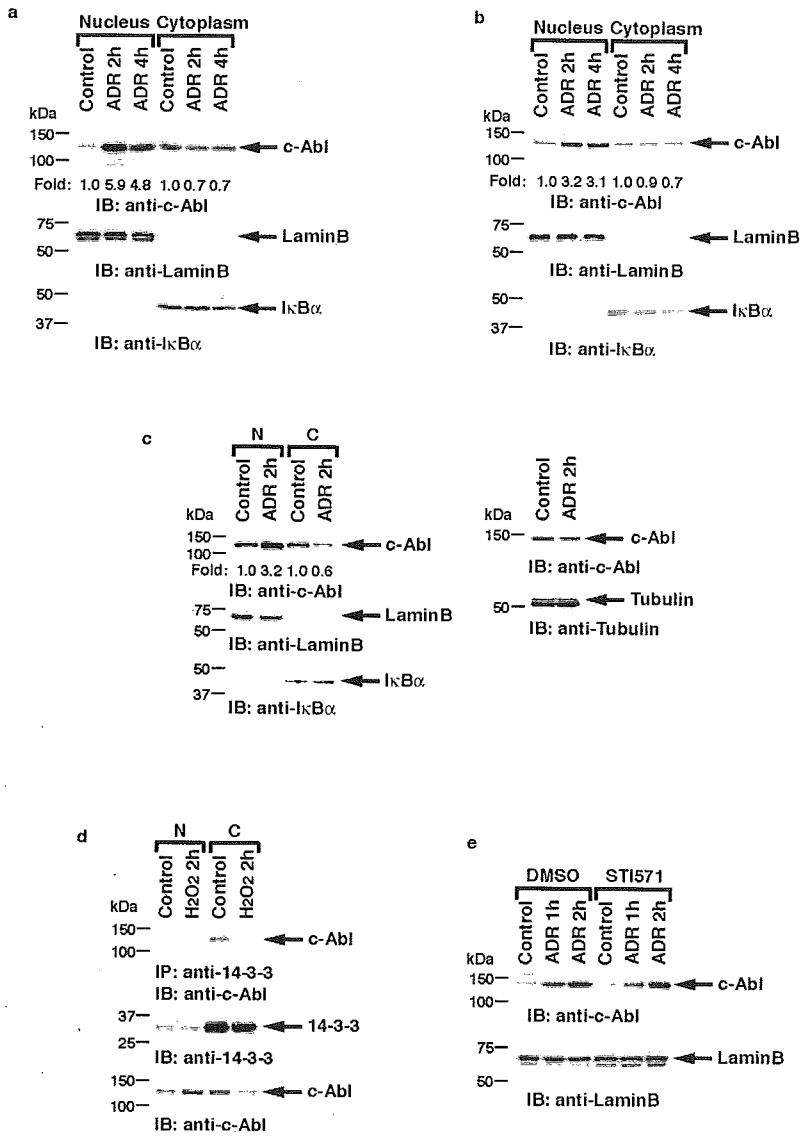

Figure S1 c-Abl translocates to the nucleus following DNA damage or oxidative stress in various cell types. (a-c) HL-60 (a), MCF-7 (b) and U-937 (c) cells were left untreated or treated with ADR for the indicated times. Nuclear and cytoplasmic lysates were analyzed by immunoblotting with anti-c-Abl (upper panel), anti-LaminB (middle panel) or anti-IκBα (lower panel). Whole cell lysates from U-937 cells were subjected to immunoblot analysis with anti-c-Abl (right, upper panel) or anti-Tubulin (right, lower panel). (d) U-937 cells were treated with 50 μM hydrogen peroxide (H_2O_2) for 2 h. Nuclear and cytoplasmic lysates were subjected to immunoprecipitation with anti-14-3-3 and then immunoblot analysis with anti-c-Abl (upper panel). Lysates were also analyzed by immunoblotting with anti-14-3-3 (middle panel) or anti-c-Abl (lower panel). (e) Kinase activity is dispensible for nuclear targeting of c-Abl in response to DNA damage. HeLa cells were treated with DMSO or 10 μM STI571 for 30 min followed by treatment with ADR. Cell lysates were subjected to immunoblot analysis with anti-c-Abl (upper panel) or anti-LaminB (lower panel).

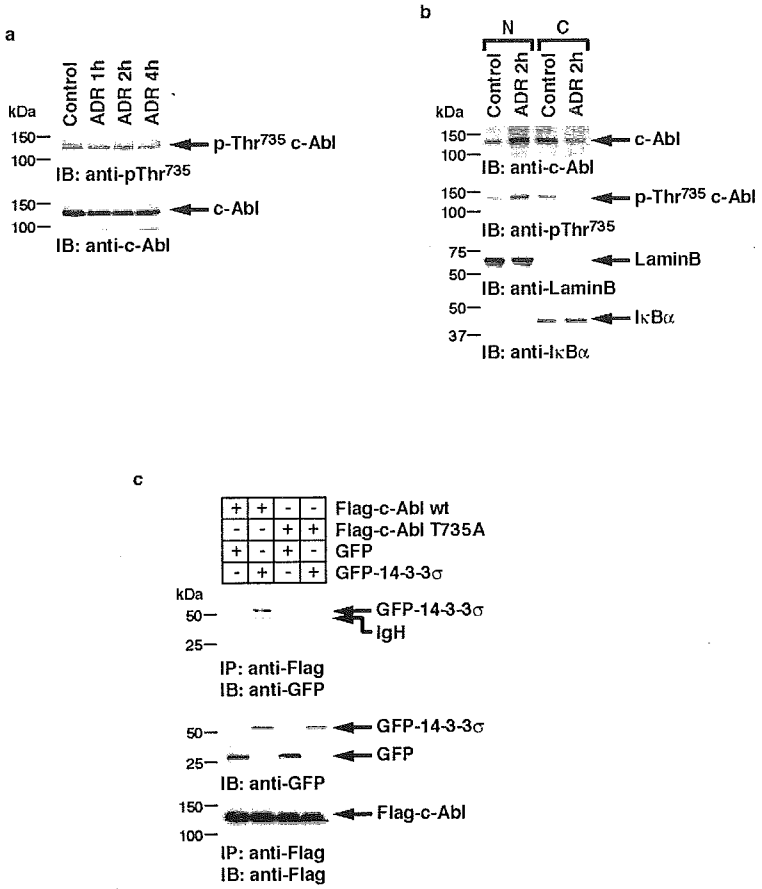

Figure S2 Thr735 in c-Abl is the major binding target for 14-3-3. (a) HeLa cells were left untreated or treated with ADR for the indicated times. Cell lyates were subjected to immunoblot analysis with anti-phospho-c-Abl (Thr735) (upper panel) or anti-c-Abl (lower panel). (b) HeLa cells were left untreated or treated with ADR for 2h. Cell lysates from nuclear and cytoplasmic fractions were analyzed by immunoblotting with indicated antibodies. (c) 293T cells were transfected with Flag-c-Abl, Flag-c-Abl(T735A), GFP-vector or GFP-14-3-3σ. Cell lysates were immunoprecipitated with anti-Flag. The immunoprecipitates were subjected to immunoblot analysis with anti-GFP (upper panel) or anti-Flag (lower panel). Lysates were also analyzed by immunoblotting with anti-GFP (middle panel).